Biogeosciences Discuss., https://doi.org/10.5194/bg-2018-57
Manuscript under review for journal Biogeosciences
Discussion started: 28 February 2018

Biogeosciences Discussions Open Access EGU

Coral reef carbonate budgets and ecological drivers in the naturally high temperature and high total alkalinity environment of the Red Sea

Anna Roik[1,*], Till Röthig[1,+], Claudia Pogoreutz[1], Vincent Saderne[1], Christian R. Voolstra[1]

[1]Red Sea Research Center, King Abdullah University of Science and Technology, 23955 Thuwal, Saudi Arabia

[*]Current address: Marine Microbiology Group, GEOMAR Helmholtz Centre for Ocean Research, 24105 Kiel, Germany

+Current address: The Swire Institute of Marine Science, Kadoorie Biological Sciences Building, The University of Hong Kong, Pokfulam Road, Hong Kong

Correspondence to: Christian R. Voolstra (christian.voolstra@kaust.edu.sa), Anna Roik (aroik@geomar.de)

Biogeosciences Discuss., https://doi.org/10.5194/bg-2018-57
Manuscript under review for journal Biogeosciences
Discussion started: 28 February 2018

Abstract. The coral structural framework is crucial for maintaining reef ecosystem function and services. Rising seawater temperatures impair the calcification capacity of reef-building organisms on a global scale, but in the Red Sea total alkalinity is naturally high and beneficial to reef growth. It is currently unknown how beneficial and detrimental factors affect the balance between calcification and erosion, and thereby overall reef growth, in the Red Sea. To provide estimates of present-day carbonate budgets and reef growth dynamics in the central Red Sea, we measured *in situ* net-accretion and net-erosion rates (G_{net}) by deployment of limestone blocks to estimate census-based carbonate budgets (G_{budget}) in four reef sites along a cross-shelf gradient (25 km). In addition, we assessed abiotic (i.e., temperature, inorganic nutrients, and carbonate system variables) and biotic (i.e., calcifier and bioeroder abundances) variables. Our data show that aragonite saturation states (Ω = 3.65 - 4.20) were in the upper range compared to the chemistry of other tropical reef sites. Further, G_{net} and G_{budget} encompassed positive (offshore) and negative (midshore-lagoon and exposed nearshore site) carbonate budgets. Notably, G_{budget} maxima were lower compared to reef growth from undisturbed Indian Ocean reefs, but erosive forces for Red Sea reefs were not as strong as observed elsewhere. In line with this, a comparison with recent historical data from the northern Red Sea suggests that overall reef growth in the Red Sea has remained similar since 1995. When assessing reef sites across the shelf gradient, A_T correlated well and positive with reef growth (ρ = 0.9), while temperature (ρ = -0.7), pH variation (ρ = -0.8), and pCO_2 (ρ = -0.8) were weaker negative correlates. Noteworthy for this oligotrophic sea was the positive effect of PO_4^{3-} (ρ = 0.7) on reef growth. In the best-fitting distance-based linear model, A_T explained about 64 % of G_{budget}. Interestingly, parrotfish abundances added up to 78 % of the explained variation, further corroborating recent studies that highlight the importance of parrotfish to reef ecosystem functioning. Our study provides a baseline for reef growth in the central Red Sea that will be particularly useful in assessing future trajectories of reef growth capacities under current and future ocean warming and acidification scenarios.

Biogeosciences Discuss., https://doi.org/10.5194/bg-2018-57
Manuscript under review for journal Biogeosciences
Discussion started: 28 February 2018

1 Introduction

Coral reef growth is limited to warm, aragonite-saturated, and oligotrophic tropical oceans and is pivotal for reef ecosystem functioning (Buddemeier, 1997; Kleypas et al., 1999). The coral reef framework not only maintains a remarkable biodiversity, but also provides highly valuable ecosystem services that include food supply and coastal protection, among others (Moberg and Folke, 1999; Reaka-Kudla, 1997). Biogenic calcification, erosion, and dissolution cumulatively contribute to the formation of the reef framework constructed of calcium carbonate ($CaCO_3$, mainly aragonite) (Glynn, 1997; Perry et al., 2008). The balance of carbonate loss and accretion are controlled by abiotic and biotic factors: temperature, properties of carbonate chemistry (e.g., pH, total alkalinity A_T, and aragonite saturation state Ω_a), calcifying benthic communities (scleractinian corals and coralline algal crusts), as well as grazing and endolithic bioeroders (e.g., parrotfish, sea urchins, and boring sponges) (Glynn and Manzello, 2015; Kleypas et al., 2001).

Positive carbonate budgets (G_{budget}) are maintained when reef calcification produces more $CaCO_3$ than is being removed, and rely in a great part on the ability of benthic calcifiers to precipitate calcium carbonate from seawater (Tambutté et al. 2011). Calcification rates increase with higher temperature, but have an upper thermal limit (Jokiel and Coles, 1990; Marshall and Clode, 2004). In addition, A_T and Ω_a, positively correlate with calcification rates (Marubini et al., 2008; Schneider and Erez, 2006). Today's oceans are warming, which poses a potential threat to calcifying reef organisms, as high temperatures begin to exceed the thermal optima of calcifying organisms and thereby slowing down calcification (Carricart-Ganivet et al., 2012; De'ath et al., 2009; Roik et al., 2015). Simultaneously, calcification becomes energetically more costly (Cai et al., 2016; Cohen and Holcomb, 2009; Waldbusser et al., 2016), as ocean acidification decreases the ocean's pH, and hence Ω_a (Orr et al., 2005). In addition, ocean acidification stimulates destructive processes, for instance the proliferation of bioeroding endolithic organisms (Enochs, 2015; Fang et al., 2013; Tribollet et al., 2009). Negative G_{budget} are a hallmark of reef degradation due to an increased intensity or frequency of extreme climate events (Eakin, 2001; Schuhmacher et al., 2005) or local human impacts, such as pollution and eutrophication (Chazottes et al., 2002; Edinger et al., 2000). A census-based G_{budget} approach is therefore a powerful tool to assess persistence of the reef framework allowing for the comparison of global and regional trends (Kennedy et al., 2013; Perry et al., 2012, 2015). Today, 37 % of all reefs studied with the G_{budget} approach are reported to be in a net-erosional state (Perry et al., 2013). For the Caribbean, G_{budget} elucidated a 50 % decrease of reef growth compared to historical mid- to late-Holocene reef growth. Finally, recent G_{budget} studies highlight the susceptibility of marginal coral reefs to ocean warming and acidification (Couce et al., 2012), such as those in the Eastern Pacific or in the Middle East (Persian/Arabian Gulf), which exist at their environmental limits, e.g., low pH or high temperatures, respectively (Bates et al., 2010; Manzello, 2010; Riegl, 2003; Sheppard and Loughland, 2002).

Despite being characterized by high sea surface temperatures that exceed thermal thresholds of tropical corals elsewhere (Kleypas et al., 1999), the Red Sea supports a remarkable coral reef framework along its entire coastline (Riegl et al., 2012). Yet, coral core samples indicate that calcification rates have already been declining over the past

82 decades in the Red Sea and elsewhere, which is widely attributed to ocean warming (Bak et al., 2009; Cantin et al.,
83 2010; Cooper et al., 2008). In the central and southern Red Sea, present-day data show reduced calcification rates of
84 corals and calcifying crusts when temperatures peak during summer (Roik et al., 2015; Sawall et al., 2015). While
85 increasing temperatures are seemingly stressful and energetically demanding for reef calcifiers, high A_T values (~
86 2400 µmol kg^{-1}, Metzl et al. 1989) in the Red Sea are putatively beneficial for carbonate accretion (Tambutté et al.,
87 2011).
88
89 Little is known regarding the G_{budget} of Red Sea coral reefs (Jones et al., 2015). Aside from one early census-based
90 assessment of the G_{budget} for a high-latitude reef in the Gulf of Aqaba (northern Red Sea), which considered both
91 calcification and erosion/dissolution rates (Dullo et al., 1996), remaining studies only report calcification rates (Cantin
92 et al., 2010; Heiss, 1995; Roik et al., 2015; Sawall and Al-Sofyani, 2015). In the present study, we therefore set out to
93 assess abiotic and biotic drivers of reef growth, and to determine the G_{budget} for coral reefs of the central Red Sea. First,
94 to reveal the present-day carbonate chemistry in the region, we examined sites along an environmental cross-shelf
95 gradient during winter and summer. Second, we followed the census-based *ReefBudget* approach (Perry et al., 2012)
96 to estimate net carbonate production states (G_{budget}) using reef site-specific biotic parameters. To achieve this, we
97 assessed the abundances and calcification rates of major reef-building coral taxa (*Porites*, *Pocillopora*, and *Acropora*)
98 and calcareous crusts, along with the abundances and erosion rates of external macro bioeroders (parrotfish and sea
99 urchins). Also, we measured net-accretion/erosion rates (G_{net}) *in situ* using limestone blocks deployed in the reefs,
100 which captured endolithic erosion rates. Finally, we explored correlations of potential drivers on G_{net} and the overall
101 G_{budget} using the abiotic and biotic data. Hence, our study provides broad insight into reef growth dynamics and a
102 comparative baseline to assess the effects of ongoing environmental change on reef growth in the central Red Sea.
103

2 Material and Methods

2.1 Study sites and environmental monitoring

Study sites were located in the Saudi Arabian central Red Sea along an environmental cross-shelf gradient, described in detail in Roik et al. (2015) and (2016). Data for this study were collected at four sites: an offshore forereef at ~25 km distance from the coastline (22° 20.456 N, 38° 51.127 E, "Shi'b Nazar"), two midshore sites (forereef and lagoon) at ~10 km distance (22° 15.100 N, 38° 57.386 E, "Al Fahal"), and a nearshore forereef (22° 13.974 N, 39° 01.760 E, "Inner Fsar") at ~3 km distance to shore. All sampling stations were located between 7.5 and 9 m depth. In the following, reef sites are referred to as "offshore", "midshore", "midshore lagoon", and "nearshore", respectively. Abiotic variables were measured during two seasons in 2014. Temperature and $pH_{(continuous)}$ were measured continuously recorded during "winter" (10th February - 6th April 2014) and "summer" (20th June - 20th September 2014). Additionally, for 5 - 6 consecutive weeks during each of the seasons, at each station seawater samples were collected on SCUBA for the determination of inorganic nutrients and carbonate chemistry: nitrate and nitrite (NO_3^- &NO_2^-), ammonia (NH_4^+), phosphate (PO_4^{3-}), total alkalinity (A_T), and $pH_{(discrete)}$ (Table S1).

2.2 Abiotic parameters

2.2.1 Continuous data: Salinity, Temperature, pH

Conductivity-Temperature-Depth loggers (CTDs, SBE 16plusV2 SEACAT, RS-232, Sea-Bird Electronics, Bellevue, WA, USA) equipped with pH probes (SBE 18/27, Sea-Bird) were deployed at 0.5 m above the reef to collect time series data of temperature and $pH_{NBS\ (continuous)}$ at hourly intervals. Both sensors were factory-calibrated. pH probes were tested before and after deployment using NBS scale buffers (pH-7, Fixanal, Fluka Analytics, Sigma-Aldrich, Germany) and linear drift corrections were applied (Table S2).

2.2.2. Seawater samples: Inorganic nutrients and carbonate chemistry

Seawater samples were collected on SCUBA at each of the stations using 4 L cubitainers (Table S1). Simultaneously, 60 mL seawater samples were taken over a 0.45 µm syringe filter for A_T measurements. Immediately after water collection, the pH of the discrete samples $pH_{(discrete)}$ was measured potentiometrically on the NBS scale in subsamples using a portable pH probe with an integrated temperature sensor (n = 3, repeatability ± 0.006, conservative estimate error based on standard buffer measurements at 20 °C ± 0.03, Orion 4 Star Plus, Thermo Fisher Scientific, MA, USA). The probe was calibrated using NBS buffers prior to each sampling day (pH-4, pH-7 and pH-10, Fixanal Fluka Analytics, Sigma-Aldrich). Seawater samples for inorganic nutrient analyses and A_T measurement were transported on ice in the dark and were processed on the same day. Samples were filtered over GF/F filters (0.7 µm, Whatman, UK) and filtrates were frozen at -20 °C until analysis. The inorganic nutrient content (NO_3^-&NO_2^-, NH_4^+, and PO_4^{3-}) was determined using standard colorimetric tests and a Quick-Chem 8000 AutoAnalyzer (Zellweger Analysis, Inc.). A_T samples were analyzed within 2 - 4 h after collection using an automated acidimetric titration system (Titrando

888, Metrohm AG, Switzerland). Gran-type titrations were performed with a 0.01 M HCl (prepared from 0.1 HCl Standard, Fluka Analytics) at an average accuracy of ± 9 µmol kg^{-1} (SD of triplicate measurements). Carbonate chemistry parameters were calculated using A_T, $pH_{(discrete)}$ (NBS scale), total silicate, and phosphates from discrete samples; Salinity, depth, and temperature data were retrieved from CTDs, using the R package *seacarb* (Gattuso et al., 2015). Calculations were made using the *seacarb* formula for pH on the Free scale, as the best available equivalent for the NBS scale, employing the first and second dissociation constants of the carbonate system by Lueker et al. (2000) and the dissociation constants for HF and HSO_4^- of Perez and Fraga (1987) and Dickson (1990), respectively.

2.3 Net-accretion/erosion rates in limestone blocks (G_{net})

Net-accretion/erosion rates were assessed using a limestone block "assay". Blocks, cut from "coral stone" limestone, were purchased from a local building material supplier in Jeddah, KSA. Blocks (100 x 100 x 21 mm, $\rho = 2.3$ kg L^{-1}, $n = 4$) were weighed before and after deployment on the reefs, where they were exposed to the natural processes of calcification and erosion. Before weighing (Mettler Toledo XS2002S, readability = 10 mg), blocks were autoclaved and dried in a climate chamber (BINDER, Tuttlingen, Germany) at 40°C for a week. Blocks were deployed for 6 months (September 2012 - March 2013) and 12 months (June 2013 - June 2014) at six sites, including the four reef sites as well as the offshore and nearshore back reefs of the corresponding forereef sites, and for 30 months (January 2013-June 2015) in the four reef sites. Upon recovery, blocks were treated with 10 % bleach for 24 - 36 h to remove organic material. G_{net} were expressed as normalized differences of pre-deployment and post-deployment weights (kg m^{-2} y^{-1}).

2.4 Biotic parameters

To assess coral reef benthic calcifier and bioeroder communities as input data for the reef carbonate budgets, we conducted *in situ* surveys on SCUBA at each of our study sites along the cross-shelf gradient.

2.4.1 Benthic community composition

The community composition and coverage of coral reef calcifying groups was assessed during both sampling seasons on SCUBA. We surveyed benthic calcifiers and non-calcifiers and categorized them as follows: % cover total hard coral, % hard coral morphs (branching, encrusting, massive, and platy/foliose), % major reef-building coral families (Poritidae, Acroporidae, and Pocilloporidae), % cover calcareous crusts, % cover algae & sponges). For a detailed description of the benthic surveys please refer to Roik et al. (2015). In addition, benthic rugosity was assessed using the *Tape and Chain Method* (Perry et al., 2012).

2.4.2 Bioeroder populations along the cross-shelf gradient

For each reef site, we surveyed abundances and size classes of the two main groups of coral reef framework bioerorders, the parrotfishes (Scaridae) (Bellwood, 1995; Bruggemann et al., 1996) and sea urchins (Echinoidea) (Bak, 1994). Surveys were conducted on SCUBA using stationary plots (adapted from Bannerot and Bohnsack, 1986, Text S1) and line transects (n = 6 per site), respectively. Briefly, abundances of parrotfishes and sea urchins were assessed for different size classes. Abundances for all prevalent parrotfish species were assessed in six size classes, based on estimated fork length (FL; FL size classes: 1 = 5 - 14 cm, 2 = 15 - 24 cm, 3 = 25 - 34 cm, 4 = 35 - 44 cm, 5 = 45 - 70, and 6 > 70 cm). The sea urchin census targeted five size classes of the four most common bioerosive genera *Diadema*, *Echinometra*, *Echinostrephus*, and *Eucidaris*, based on urchin diameter (size classes 1 = 0 - 20 mm, 2 = 21 - 40 mm, 3 = 41 - 60 mm, 4 = 61 - 80 mm, 5 = 81 - 100 mm). For details on the field surveys and data treatment for biomass conversion, refer to the supplementary materials (Text S1 and references therein).

2.5 Reef carbonate budgets (G_{budget})

Reef carbonate budgets (G_{budget}, kg m^{-1} y^{-1}) were estimated following the census-based *ReefBudget* approach (Perry et al., 2012). Site-specific benthic calcification rates ($G_{benthos}$, kg m^{-1} y^{-1}), net-accretion/erosion rates of hard substrate ($G_{netbenthos}$, kg m^{-1} y^{-1}), and erosion rates of crucial macro bioeroders such as sea urchins (E_{echino}, kg m^{-1} y^{-1}) and parrotfishes (E_{parrot} , kg m^{-1} y^{-1}) were incorporated in the G_{budget} estimates (Fig. 1). A detailed account of Red Sea specific calculations and modifications of the *ReefBudget* approach are outlined in the supplementary materials (Text S1, Equation box S1-3, and Tables S2-6).

2.6 Statistical analyses

2.6.1 Abiotic parameters

Continuous temperature and $pH_{(continuous)}$ data were summarized as daily means, daily standard deviations (SD), and daily minima/maxima. Diel profiles were plotted per reef and season including smoothing polynomial regression lines fitted by *geom_smooth* in R package *ggplot2* (LOESS, span = 0.1). Data were additionally visualized in histograms using the function *stat_bin*, as implemented in the R package *ggplot2* (R Core Team, 2013; Wickham and Chang, 2015). Univariate 2-factorial permutational ANOVAs (PERMANOVAs, PRIMER-E V6) were used to test the factors "reef" (nearshore, midshore lagoon, midshore, and offshore) and "season" (winter and summer). PERMANOVAS were performed on Euclidian resemblance matrices calculated from $log_2(x+1)$ transformed data (Anderson et al., 2008) and were based on 999 permutations of residuals under a reduced model and type II partial sums of squares. Within each significant factor, pair-wise PERMANOVA tests followed. Then, inorganic nutrients (NO_3^-&NO_2^-, NH_4^+, and PO_4^{3-}) which fulfilled parametric assumptions were evaluated using univariate 2-factorial ANOVAs under the same test design. Analyses were not performed on the carbonate system estimates, which show a large uncertainty based on the precision of the pH measurements (SD between 0.018 and 0.051).

205 **2.6.2 Net-accretion/erosion rates and carbonate budgets**

206 G_{net} data were tested for effects of the factors "reef" (nearshore, midshore, and offshore), "site exposure" (forereef and
207 backreef/lagoon), and "deployment time" (6, 12, and 30 months). Because of an incomplete design due to the missing
208 nearshore and offshore backreef sites in the 30-months deployment, a univariate 3-factorial PERMANOVA was
209 conducted using Euclidian distance matrix 999 permutations of residuals under a reduced model and type II partial
210 sum of squares.
211
212 G_{budget} were tested for statistical differences between the four "reef sites" (nearshore, midshore lagoon, midshore, and
213 offshore) using a 1-factorial ANOVA, after box-cox transforming the data to meet test assumptions. In parallel, biotic
214 variables were tested using a 1-factorial ANOVA for square-root transformed $G_{benthos}$, and non-parametric Kruskal-
215 Wallis tests for non-transformed $G_{netbenthos}$, E_{echino}, and E_{parrot}. Tukey's HSD post-hoc tests followed where applicable.
216

217 **2.6.3 Abiotic-biotic correlations**

218 To evaluate the relationship of abiotic and biotic predictors of G_{net} and G_{budget}, a multivariate statistics approach was
219 applied. Distance-based linear models (DistLM) were performed including biotic and abiotic predictor variables
220 (PRIMER-E V6). Models were tested for (a) G_{net} and (b) G_{budget} data. G_{net} encompassing data obtained in the 30-
221 months measurements from four reef sites (nearshore, midshore lagoon, midshore, and offshore). Predictor variables
222 in (a) and (b) were 13 reef growth-relevant abiotic parameters, comprising means and SDs from continuous
223 measurements of temperature and $pH_{(continuous)}$ per reef site, the means of inorganic nutrients (NO_3^-&NO_2^-, NH_4^+, and
224 PO_4^{3}), and means of carbonate chemistry parameters (A_T, C_T, Ω_a, HCO_{3^-}, CO_3^2, and pCO_2, also see Table 1). (a) The
225 G_{net} model included only three of the biotic variables which potentially had influence on the limestone blocks, i.e.
226 parrot fish abundances, calcareous crusts cover, and algal and sponge cover. (b) G_{budget} models included all 13 biotic
227 transect variables (i.e., parrot fish abundances, sea urchin abundances, % branching coral, % encrusting coral, %
228 massive coral, % platy/foliose coral, % of Acroporidae, % Pocilloporidae, % Poritidae, % total hard coral cover,
229 calcareous crusts cover, algal and sponge cover, and rugosity). Prior to DistLM, some of the predictor variables (i.e.,
230 sea urchin and parrotfish abundances, % platy/foliose corals, and % Poritidae) were $\log_{10}(x+1)$ transformed to improve
231 the symmetry in their distributions following (Anderson et al., 2008). Both DistLM routines were performed on
232 Euclidian resemblance matrices, implementing the step-wise forward procedure with 9999 permutations and adjusted
233 R^2 criterion. Additionally, Spearman rank correlation coefficients were obtained for the predictor variables (at an
234 confidence level of 95%) using *cor.test* in R (R Core Team, 2013; Wickham and Chang, 2015).
235

Biogeosciences Discuss., https://doi.org/10.5194/bg-2018-57
Manuscript under review for journal Biogeosciences
Discussion started: 28 February 2018

3 Results

3.1 Abiotic parameters relevant for reef growth

3.1.1 Temperature and pH

The seasonal mean temperature varied between 26.0 ± 0.6°C in winter and 30.9 ± 0.7°C in summer across all reefs (Table 1). The difference across the shelf was on average ~0.4°C (Table S10). The nearshore and midshore reefs experienced the lowest (both ~26°C in winter), and the nearshore reef the highest mean temperatures (31.5 ± 0.6°C in summer). Seasonal and spatial differences in all temperature data (daily means, daily SDs, daily minima and maxima) were significant (Fig. 2 (a) - (b), Table S11). Compared to all other sites, the nearshore reef experienced significantly higher daily maxima during summer ("daily max.", $p = 0.01$, Fig. 2 (a), Table S10), and significantly lower minima during winter ($p < 0.01$, see also Table S11).

Across all reef sites, seasonal means for $pH_{(continuous)}$ were 8.13 ± 0.19 in winter and 8.15 ± 0.13 in summer (Table 1). Lowest seasonal means were recorded on the midshore lagoon with 8.00 ± 0.17 in winter and 8.09 ± 0.22 in summer, and highest in the nearshore reef (8.25 ± 0.27 in winter and 8.31 ± 0.12 in summer). $pH_{(continuous)}$ was intermediate on the exposed midshore and offshore (8.10 ± 0.05 to 8.16 ± 0.09). Overall, $pH_{(continuous)}$ data showed that spatial differences were more pronounced (with a mean difference between site averages of 0.15 pH units, Table S10), compared to a minor effect of seasonality (with a mean difference between seasonal averages of 0.02 pH units). $pH_{(continuous)}$ followed a diel pattern with peak values around solar noon (12:36 h MST) in nearshore and midshore lagoon. This peak was shifted towards 14:00 - 15:00 h in the midshore and offshore exposed sites. All diel $pH_{(continuous)}$ variables differed between reef sites ($p < 0.01$, Table S11, Fig. 2 (c) and (d)). Diel-$pH_{(continuous)}$ SDs and maxima were significantly different between the seasons ($p < 0.01$ and $p < 0.05$, respectively). Notably, the diel $pH_{(continuous)}$ ranges were small in the exposed offshore and midshore site (0.05 - 0.09 SD pH units, Table 1), while the lagoon and nearshore reef was characterized by a larger diel SDs (0.12 - 0.27 pH units).

3.1.2 Inorganic nutrients and carbonate chemistry

Inorganic nutrients showed a major variation between the seasons (both $p < 0.001$, Table S11). Specifically, NO_3^- &NO_2^- and NH_4^+ levels were higher in winter (0.32 ± 0.18 µmol kg^{-1} and 0.44 ± 0.37 µmol kg^{-1}) compared to summer (0.61 ± 0.24 µmol kg^{-1} and 0.54 ± 0.30 µmol kg^{-1}). In contrast, PO_4^{3-} was higher in winter than in summer (0.07 ± 0.02 vs. 0.04 ± 0.04 µmol kg^{-1}, Table 1, Table S11 and Fig. 3 (a)). Highest inorganic nutrient contents were measured in the midshore lagoon with up to 0.92 µmol NO_3^-&NO_2^- kg^{-1}, 1.59 µmol NH_4^+ kg^{-1} in summer, and 0.09 µmol PO_4^{3-} kg^{-1} in winter, but PO_4^{3-} was also high in the offshore reef during winter (0.12 µmol PO_4^{3-} kg^{-1}).

During winter, A_T, C_T, and HCO_3^- concentrations were elevated (2422 µmol A_T kg^{-1}, 2076 µmol C_T kg^{-1}, and 1821 µmol HCO_3^- kg^{-1}) compared to summer (2369 A_T µmol kg^{-1}, 2005 µmol C_T kg^{-1}, and 1740 µmol HCO_3^- kg^{-1}, Table 1, Fig. 3 (b), Table S11). Conversely, mean Ω_a and CO_3^{2-} were overall reduced during winter (winter: 3.77 Ω_a and 244

µmol CO_3^{2-} L^{-1}; summer: 4.00 Ω_a and 254 µmol CO_3^{2-} L^{-1}). Estimates of pCO_2 in this study ranged 414 - 468 µatm across reef and seasons. By trend, A_T and Ω_a increase from nearshore to offshore (Fig. 3 (b)). Of note, the precision on the measured pH (± 0.03) and A_T (± 10) propagates to uncertainty in the calculated parameters of the carbonate system, resulting in a mean accuracy for Ω_a, pCO_2, C_T and CO_3^{2-} being ± 0.21, ± 36 µatm, ± 11 µmol kg^{-1}, and ± 14 µmol kg^{-1}, respectively.

3.2 Biotic parameters relevant for reef growth

3.2.1 Benthic community composition

A low percentage of live substrate (< 40 %) was characteristic of the backreef/lagoonal sites. In exposed ocean facing sites of the offshore and midshore reefs a community of calcifying organisms took up to 48 % of benthos cover on average (hard corals and calcareous crusts). Major reef-building corals were the genera *Acropora*, *Pocillopora*, and *Porites* constituting 32 - 56 % of the total hard coral cover. A detailed account of benthic community structure of the study sites is provided in Roik et al. (2015) and the mean values used for the calculation of benthic accretion rates ($G_{netbenthos}$ kg m^{-2} y^{-1}) for the G_{budget} estimation are presented in Tables S2-3.

3.2.2 Abundances and biomasses of macro bioeroders

A total of 718 parrotfishes and 110 sea urchins were observed in the present study. For sea urchins, mean abundances and biomass estimates of 0.002 ± 0.004 - 0.014 ± 0.006 individuals m^{-2} and 0.05 ± 0.04 - 1.43 ± 0.98 g m^{-2} were observed, respectively (Table S5). Parrotfish mean abundances and biomass estimates ranged from 0.05 ± 0.01 - 0.17 ± 0.60 individuals m^{-2} and 19.54 ± 5.56 - 82.18 ± 46.67 g m^{-2}, respectively (Table S7). The highest abundances and biomasses of both parrotfishes and sea urchins were observed at the exposed nearshore site. Abundances and biomasses of these two bioeroding groups decreased towards the exposed midshore site, and then increased again towards the exposed offshore site. All backreef sites and the exposed midshore site exhibited the largest range of sea urchin size classes (from categories 1 or 2 to the largest size class 5), while at the other two exposed sites, only the two smallest size classes of sea urchins were recorded. The largest parrotfishes (category 5 parrotfish, i.e., > 45 - 69 cm fork length) were observed at the midshore sites and the backreef offshore site. With the exception of the exposed midshore reef, category 1 (5 - 14 cm) parrotfish were commonly observed at all sites. In contrast, no category 6 parrotfish (≥ 70 cm fork length) were observed during the surveys.

3.3 Net-accretion/erosion rates

Cumulative net-accretion/erosion rates G_{net} were measured in assays over 6, 12, 30 months in the reef sites along the cross-shelf gradient. Visible boring traces of endolithic worms or sponges were only found on the surfaces of blocks recovered after 12 and 30 months (Fig. 4 (c)-(j)). G_{net} based on the 30-months deployment of blocks ranged between

-0.96 and 0.37 kg m^{-2} y^{-1} (Table 2). G_{net} for 12 and 30-months blocks were negative on the nearshore reef (between -0.96 and -0.2 kg m^{-2} y^{-1}, i.e., net erosion is apparent), near-zero on the midshore reef (0.01 - 0.06 kg m^{-2} y^{-1}, i.e., low net accretion), and positive on the offshore reef (up to 0.37 kg m^{-2} y^{-1}, i.e., high net accretion). Reef sites and deployment times had a significant effect on the variability of G_{net} (Table S12). As expected, accretion/erosion was overall higher when measured over the longest deployment period ($p < 0.001$, Fig. S1) and compared to shorter deployment times, reflecting the continuous and exponential nature of bioerosion due to the colonization progress of fouling organisms over time.

3.4 Carbonate budgets

The carbonate budget G_{budget}, estimated via the *ReefBudget* approach (Perry et al., 2012) and averaged over all sites was 0.65 ± 1.73 kg m^{-2} y^{-1}. This average encompasses values from the negative nearshore budget -1.48 ± 1.75 kg m^{-2} y^{-1} to the positive offshore budget 2.44 ± 1.03 kg m^{-2} y^{-1} (Table 3). G_{budget} significantly differed between the reef sites ($p < 0.05$, Fig. 5 (a)), except for budgets in both midshore sites (lagoon and exposed), which were similar. Biotic variables that account for the carbonate budgets also differed by site, in the case of community calcification rates $G_{benthos}$ ($p < 0.05$, Fig. 5 (b)), and net-accretion/erosion of bare substrate $G_{netbenthos}$ ($p < 0.001$, Fig. 5 (c)). However, differences of parrot fish and echinoid erosion rates (E_{echino} and E_{parrot}) were not significant (Fig. 5 (d) - (e)).

3.5 Abiotic and biotic drivers related to net-accretion rates and carbonate budgets

Spearman rank correlations and distance based linear models show similar results for G_{net} and G_{budget}. First correlations show that temperature means, temperature SDs, and $pH_{(continuous)}$ SDs, and pCO_2 were negatively correlated, while A_T, Ω_a, CO_3^{2-}, and PO_4^{3-} were positively correlated with both reef growth variables ($\rho \geq |0.6|$, Table 4). Among biotic variables, calcareous crusts and % total hard coral were positively correlated with G_{net} and G_{budget}. Second, the best distance-based linear model for G_{net} data accounted for 65 % (adjusted R^2) of the total variation. Here, A_T alone explained 65 % of the G_{net} data and was the only statistically valid predictor (Table 5). The best model for G_{budget} fitted two biotic and two abiotic predictors and explained total variation of 81 % (adjusted R^2). Again, A_T was the major predictor explaining 64 % alone. The biotic variable 'parrotfish abundance' added up to 78 % of explained variation. Both variables were statistically significant in the test. The remaining predictors included in the model ($pH_{(continuous)}$ SD and % encrusting coral) were non-significant and of minor relevance (altogether contributing only 3 %, Table 5).

Biogeosciences Discuss., https://doi.org/10.5194/bg-2018-57
Manuscript under review for journal Biogeosciences
Discussion started: 28 February 2018

4 Discussion

The Red Sea is governed by unique environmental conditions of high salinity and temperature. So far, reef growth in the Red Sea has mostly been investigated regarding the effect of high temperature on calcification rates of reef-building corals (Cantin et al., 2010; Roik et al., 2015; Sawall et al., 2015). In this study we present the first comprehensive estimate of reef carbonate budgets for the central Red Sea. To do this, we collected environmental data of abiotic and biotic variables affecting present-day reef growth. We link calcification data on an ecosystem scale with a range of abiotic and biotic variables (carbonate chemistry and nutrient availability; abundance and activity of major bioeroders, respectively) by applying a census-based carbonate budget (G_{budget}) approach following Perry et al. (2012). Our approach integrates the net-accretion/erosion rates (G_{net}) of six reef sites along the cross-shelf gradient assessed *in situ* using a limestone block assay. In the following, we discuss central Red Sea reef growth rates (spanning from net-erosive states nearshore to net-accretion in the midshore and offshore reefs) in the context of the prevailing abiotic and biotic drivers. Finally, we discuss our results in a global and historical context.

4.1 Carbonate system and abiotic factors governing reef growth in the central Red Sea

Reef environments in the region are characterized by high salinity (38 – 39) and high summer temperatures (29 - 33 °C) coupled with low dissolved oxygen levels (2 - 4 mg L^{-1}, Roik et al., 2016) that are regarded as factors that deviate from the typical tropical reef environment in which a majority of coral reefs exist. The present study provides measurements of reef water carbonate chemistry alongside with calcification, erosion, and reef carbonate budgets adding new information to our knowledge of these Red Sea reef habitats. Regarding the carbonate system parameters presented here, it needs to be considered that the calculated accuracy of our pH measurements, ± 0.03, is close but above the "weather goal" of ± 0.02 as defined by Bockmon and Dickson (2015). Notably, the propagated error of the $pH_{(discrete)}$ measurements through the carbonate system calculations converts into an error of approximately ± 0.21 in Ω_a, ± 36 µatm pCO_2. Still, we observe that aragonite saturation states are higher than on several Pacific and Caribbean reefs (Table 6), while the mean calculated pCO_2 (414 to 468 µatm, Table 1) is similar in this comparison, and also near the reported atmospheric values (accessed November 2017: 405.58 µatm pCO_2; NOAA/Earth System Research Laboratory). The high Ω_a can be attributed to the salinity and A_T of the Red Sea, ranging from 2346 - 2429 µmol kg^{-1} (Table 1), supporting the notion that Red Sea reefs could be a refuge for reef-building corals under climate change with respect to ocean acidification (OA) (Camp et al., 2018). To test the hypothesis whether Red Sea reefs will reach a critically low Ω_a later, and maintain a calcification-friendly sea water chemistry on longer terms, compared to other tropical reef regions under OA, an experimental approach and a high precision and high resolution monitoring of reef carbonate chemistry are needed.

The present study further indicates that carbonate system variables and inorganic nutrients vary on temporal (seasonal, diel) and spatial scales (cross-shelf gradient, exposed/sheltered reef sites). Similarly, seasonality of the carbonate system was observed at the high latitude reefs of the GoA (Gulf of Aqaba), where A_T and C_T decrease while Ω_a increase during summer (Silverman et al., 2007a). While seasonal dynamics of inorganic nutrient concentrations have

been shown by remote sensing data for the entire Red Sea basin (Raitsos et al., 2013), the present study demonstrates such dynamics on local reef scale, which again was similar to seasonality in the northern reefs of the GoA (Bednarz et al., 2015). Noteworthy for our study sites was a PO_4^{3-} enrichment during winter.

Diel $pH_{(continuous)}$ fluctuation is the consequence of benthic biotic processes, i.e., calcification, dissolution, and respiration/photosynthesis that influence the amount and speciation of DIC, also referred to as biotic feedback (Bates et al., 2010; Silverman et al., 2007a; Zundelevich et al., 2007). For reference of scale, the diel pH variation measured on various coral reefs across the globe can be observed between ~7.80 to ~8.20 pH, spanning a range of ~0.4 pH units, (Albright et al., 2013; Silbiger et al., 2014). Amongst the range maxima of pH units was ~1.40 (Hofmann et al., 2011). In the present study, the diel $pH_{(continuous)}$ was less variable in the exposed midshore and offshore site reflecting a weaker biotic feedback, which was likely buffered by the higher rates of reef water mixing with the open sea water (Roik et al., 2016). In contrast, observed variation in diel $pH_{(continuous)}$ in the midshore lagoon and nearshore reefs was larger. The diel $pH_{(continuous)}$ variations suggest potential co-fluctuation of A_T and C_T that can impact calcification rates at daily time scales, but were not considered in this study. However, these highly variable nearshore and midshore lagoonal reefs from the present study offer suitable study sites to further investigate these small-scale processes (*sensu* Camp et al., 2017; Cyronak et al., 2014; Page et al., 2016).

Despite the error associated with the carbonate system calculations, we report averages differences between nearshore to offshore A_T (15 - 47 µmol kg^{-1}) and Ω_a (0.15 – 0.27) for the cross-shelf gradient (Table S10). The difference in A_T is similar to cross-shelf differences reported from e.g. reefs in Bermuda (20 - 40 µmol A_T kg^{-1}, Bates et al., 2010). Calcification and dissolution feedback, as well as water circulation patterns may explain these spatial gradients: The offshore and midshore reefs receive currents from the Red Sea basin (Roik et al., 2016), which supplies A_T saturated open sea water to the reefs. In contrast, the nearshore reef and midshore lagoon are mostly supplied by the boundary current from the south travelling along the coastal reef systems which deplete its A_T.

The differences in seawater chemistry between offshore and nearshore reefs correlated to reef growth processes: the most striking negative correlates were mean temperatures, $pH_{(continuous)}$ variability, and pCO_2, while carbonate system parameters indicative of carbonate ion availability, i.e. A_T, Ω_a, CO_3^{2}, and also a nutrient, i.e., PO_4^{3-}, were positively related to reef growth. The negative correlates reflect that higher mean temperatures and the impact of strong biotic feedbacks causing pH fluctuations govern nearshore habitats of low reef growth capacity. Previously, pH fluctuation on the micro-habitat scale has been shown to have a significant impact on accretion and erosion dynamics on coral reefs (Silbiger et al., 2014). Potentially these conditions physiologically challenge reef-building organisms, as they exert negative effects on the reef growth rate. The positive effect of high A_T, Ω_a, and CO_3^{2-} on the calcification process is well known from laboratory experiments and manipulations on reef communities *in situ* (Langdon et al., 2000, Schneider and Erez, 2006, Silverman et al., 2007b, Bates et al., 2010). Indeed, in the present study, A_T was the strongest predictor for both G_{net} and G_{budget}, alone explaining more than half of the variation in reef growth rates. Interestingly, our study also identifies PO_4^{3-} concentration, an essential macronutrient and important source of energy

406 for primary producers and reef calcifiers (Ferrier-Pagès et al., 2016), to be a strong abiotic correlate of reef growth.
407 While an overload of inorganic nutrients can be detrimental for the calcification process (Fabricius, 2005; Tambutté
408 et al., 2011), our results show that in a highly oligotrophic reef system such as the Red Sea, reef growth might be
409 positively affected by seasonal increases in PO_4^{3-} levels. Experimental studies have shown that PO_4^{3-} provision can
410 help maintain the coral-algae symbiosis in reef-building corals that suffer from heat stress (Ezzat et al., 2016) and,
411 conversely, phosphorus limitation can increase the stress susceptibility of the coral-algae symbiosis (Pogoreutz et al.,
412 2017; Rädecker et al., 2015; Wiedenmann et al., 2013). In the light of our results, it will be of interest to further study
413 spatio-temporal variation of inorganic nutrient ratios to understand their effects on large-scale and long-term trends
414 of reef growth in the central Red Sea.
415

416 **4.2 Biotic factors governing reef growth in the central Red Sea**

417 Calcifying benthic communities contribute to carbonate production and are considered the most influential drivers for
418 G_{budget} on global scale (Franco et al., 2016). Loss of coral cover rapidly gives way to increased bioerosion as the critical
419 force of degradation of the carbonate reef framework. This has become particularly apparent in the Caribbean, where
420 G_{budget} were reported to shift into negative production states when live hard coral cover was below 10 % (Perry et al.,
421 2013). Similarly, the relevance of benthic calcifying communities (coral and coralline algae) was highly apparent in
422 the present dataset from the central Red Sea: benthos cover percentage of total hard coral and calcareous crusts
423 constituted the strongest positive correlates for G_{budget}, and the latter particularly for the variable G_{net}.
424

425 Previous studies demonstrated that the community composition and abundance of bioeroders potentially influence
426 reef carbonate budgets (Alvarez-Filip et al., 2009; Bak, 1994; Bellwood, 1995; Bronstein and Loya, 2014;
427 Bruggemann et al., 1996). We show that parrotfish abundance was a considerable driving force across our study sites
428 explaining ~20 % of G_{budget} data variation. The ecological role of parrotfish grazing is the regulation of benthic algal
429 growth, supporting the recruitment of reef calcifiers, hence helping maintain a coral-dominated state (Mumby, 2006).
430 Removal of algal turfs by parrotfish has even further implications down to microbial scales (e.g., reduction of putative
431 pathogens, Zaneveld et al., 2016). On undisturbed coral reefs, parrotfishes comprise several herbivorous functional
432 groups with differential capabilities to remove algal turfs/macroalgae and/or coral reef framework (Green and
433 Bellwood, 2009). Consequently, low parrotfish abundances would on the one hand reduce erosion pressure on a reef,
434 but on the other hand may promote phase-shifts to non-calcifying organisms, such as fleshy macroalgae (Hughes et al
435 2007). In the long term, this can cause a decrease in gross carbonate production. Moreover, overfishing of
436 (parrot)fishes can reduce feeding pressure on bioeroders or their larvae (e.g., sea urchins), resulting in an uncontrolled
437 population increase leading reefs on a trajectory of degradation (Edgar et al., 2010; McClanahan and Shafir, 1990). In
438 the present study, parrotfish biomasses were lowest at the sheltered midshore site, and increased towards nearshore
439 and offshore. Such differences can be attributed to natural (e.g., species distribution, habitat preferences, reef rugosity)
440 and/or anthropogenically-driven factors (e.g., differential fishing pressure; McClanahan, 1994; McClanahan et al.,
441 1994). Indeed, the Saudi Arabian central Red Sea is subject to decade-long unregulated fishing pressure, which has

significantly altered overall reef fish community structures and reduced overall fish biomass compared to less impacted regions in the Red Sea (Kattan et al., 2017).

4.3 Cross-shelf patterns of net accretion/erosion rates and carbonate budget estimates

The G_{budget} estimates herein represent the cumulative contribution of the major biotic drivers of reef growth, i.e., $G_{benthos}$, $G_{netbenthos}$, E_{echino} and E_{parrot}, at each site (Glynn, 1997; Perry et al., 2012). Importantly, we observed a net-erosive budget in the nearshore reef, a low net-accretion (near zero) in the midshore reef, and a high net-accretion budget in offshore. Following the accretion increase across reef sites from nearshore to offshore, our G_{budget} estimates imply that nearshore reefs currently erode with half the speed that the offshore reefs grow, which may be interpreted as the formation of an offshore barrier reef in the central Red Sea (see Fig. 5 (a)). In this regard, our measured G_{net} rates from the nearshore reefs show that net-erosion states in the Red Sea reefs are less pronounced than the most extreme erosive scales reported from e.g. Moorea or the Andaman Sea, where lowest values were ~ -7 to -4 kg m^{-2} y^{-1} (Pari et al., 1998; Schmidt and Richter, 2013).

The cross-shelf dynamics of G_{budget} and the biotic drivers (Fig. 5 (b) - (e)) are complex and follow unique patterns that are in parts distinct from what we know from other reef systems. Other than observed on the GBR, where reef growth is reported to be high at inshore reefs (Browne et al., 2013), the central Red Sea nearshore study site was net-erosive. Also, parrotfish erosion was highest in the nearshore area in the present study, whereas lower rates were reported for the inshore reefs in the GBR (Hoey and Bellwood, 2007; Tribollet et al., 2002). On Caribbean islands, parrotfish erosion rates are higher in leeward reefs (that are similar to protected nearshore habitats), but these sites are typically characterized by a high coral cover which drives a positive G_{budget} (Perry et al., 2012, 2014). This is in contrast to the central Red Sea nearshore reef, which had the highest parrotfish erosion, but a negative G_{budget} due to low coral cover. This inter-regional comparison demonstrates that patterns encountered in one cross-shelf reef system cannot necessarily be readily extrapolated to another system. In conclusion, *in situ* studies will be required for each unique system to understand its dynamics and its responses to environmental change.

4.4 Global and historical perspective on reef growth in the Red Sea

The central Red Sea G_{budget} are comparable with the majority of reef sites in the Caribbean, eastern and central western Pacific ranging from -0.8 to 4.5 kg m^{-2} y^{-1} (Mallela and Perry, 2007). The highest G_{budget} from the central Red Sea are in the range of average global reef growth. However, central Red Sea reefs do not reach highest accretion estimates reported, e.g., from the remote reefs in the Indian Ocean at the Chagos Archipelago which hold a record of up to 9.8 kg m^{-2} y^{-1} G_{budget} (Perry et al., 2015).

Due to the lack of comparative data, it remains difficult to draw a historical perspective on G_{budget} in the central Red Sea. Among the data available are pelagic and reefal net carbonate accretion rates, estimated using basin-scale

historical measurements of A_T from 1998 (Steiner et al., 2014). Another data set is the census-based budget approach from a fringing reef in GoA from 1994 - 1996 (Dullo et al., 1996). The A_T-based reef accretion estimate from 1998 (0.9 kg $m^{-2}y^{-1}$) and the GoA fringing reef budget from 1994 - 1996 (0.7-0.9 kg $m^{-2}y^{-1}$) both provide similar estimates. G_{budget} assessed in the present study are in accordance with these historical data supporting the notion of stable reef growth rates in the Red Sea in recent times. Additionally, the gross calcification rate of benthic communities ($G_{benthos}$) from our offshore site compares well with the maxima measured in GoA reefs in 1994, i.e., 2.7 kg m^{-2} y^{-1} (Heiss, 1995).

The available data from the Red Sea region suggest that coral reef growth might have not changed over the past 20 years despite the ongoing warming trend (Raitsos et al., 2011). However, any comparison between the central Red Sea and GoA should be interpreted with caution. Due to differences in seasonal patterns along with the strong latitudinal gradient of temperature and salinity between the central Red Sea and GoA, reef growth dynamics from the two regions may differ and introduce bias. Increasing warming rates of sea surface temperatures since 1990 coincided with decreasing coral calcification rates in the central Red Sea (Cantin et al., 2010). It thus remains to be determined whether a declining calcification capacity has an impact on the overall reef growth and whether this phenomenon can be observed along the entire north-south gradient of the Red Sea basin. In this context, the data presented in this study will serve as a valuable baseline for comparative future studies in the central Red Sea region. Importantly, these data were collected before the Third Global Bleaching Event, which impacted the region during summer 2015 (Monroe et al., accepted) and 2016. Our report will be of great value when assessing potential (long-term) changes in the Red Sea G_{budget} after this significant disturbance.

5 Conclusions

The Red Sea is a geographic region where coral reefs exist in a naturally high temperature and high salinity environment. Baseline data for reef growth from this region are particularly valuable as they provide insight into reef functioning that deviate from the global average for coral reefs, and can potentially provide a window into future ocean scenarios. Our study is the first to provide 1) foundation data on pH dynamics and carbonate system estimates of central Red Sea reefs over two seasons of the year that are linked with 2) an assessment of growth rates of the very same reefs. We show that reef growth dynamics are positively influenced by A_T and Ω_a, which are maintained at high levels in the Red Sea, but also by the presence of phosphate, which is scarce in this oligotrophic system. Further, as suggested for other reef sites globally, our data indicate that reef growth in the Red Sea is sensitive to increasing temperature, pH variation, and pCO_2. However, to predict the exact trajectories of the carbonate system balance in the Red Sea reefs under future ocean acidification scenarios, more precise and frequent measurements of seawater chemistry are required. Nevertheless, our reef carbonate budget estimates provide a first understanding of Red Sea reef growth across geographic and temporal scales. Our data suggest that reef growth on Red Sea offshore reefs is not higher than but comparable to reef growth estimates of other regions. Interestingly, the erosive forces in the Red Sea are not as pronounced as observed elsewhere. A first comparison with recent historical data suggest that reef growth

rates in the Red Sea might not have decreased over the past few decades, despite warming, and this calls for more detailed investigations into the parameters affecting Red Sea reef growth. Projecting forward, our study provides an important baseline for evaluating the impact of ongoing and future disturbances, such as the most recent high temperature anomalies of 2015/16.

Acknowledgements

We thank the Coastal and Marine Resources Lab (CMOR) at King Abdullah University of Science and Technology (KAUST) for logistics and operations at sea (E. Al-Jahdali, A. Al-Jahdali, G. Al-Jahdali, R. Al-Jahdali, H. Al-Jahdali, F. Mallon, P. Müller, and D. Pallett), as well as for the assistance with the deployment of oceanographic instruments (L. Smith, M.D. Pantalita, and S. Mahmoud). We would like to acknowledge field assistance by C. Roder and C. Walcher in setting up the monitoring sites. Research reported in this publication was supported by funding to CRV from King Abdullah University of Science and Technology (KAUST).

Data availability.

Relevant data are within the paper and its Supplementary materials file. In addition, physicochemical raw data is available from the Dryad Digital Repository *(will be included after review)*

Supplement link. The Supplementary material related to this article is available online *(will be included by Copernicus)*

Author contribution

Resources: CRV
Project administration: CRV
Conceptualization: AR
Investigation: AR TR CP
Methodology: AR TR CP
Formal analysis: AR CP VS
Validation: AR CP TR VS CRV
Visualization: AR
Funding acquisition: CRV
Writing - original draft: AR
Writing – review & editing: CRV TR CP VS AR
Data curation: AR

Competing interests

The authors declare that they have no conflict of interest.

548 **References**

549 Albright, R., Langdon, C. and Anthony, K. R. N.: Dynamics of seawater carbonate chemistry, production, and
550 calcification of a coral reef flat, Central Great Barrier Reef, Biogeosciences Discuss., 10, 7641–7676,
551 doi:10.5194/bgd-10-7641-2013, 2013.

552 Alvarez-Filip, L., Dulvy, N. K., Gill, J. A., Côté, I. M. and Watkinson, A. R.: Flattening of Caribbean coral reefs:
553 region-wide declines in architectural complexity, Proc. R. Soc. Lond. B Biol. Sci., 276(1669), 3019–3025,
554 doi:10.1098/rspb.2009.0339, 2009.

555 Anderson, M. J., Gorley, R. N. and Clarke, K. R.: PERMANOVA+ for PRIMER: Guide to software and statistical
556 methods, 2008.

557 Bak, R. P. M.: Sea urchin bioerosion on coral reefs: place in the carbonate budget and relevant variables, Coral Reefs,
558 13(2), 99–103, doi:10.1007/BF00300768, 1994.

559 Bak, R. P. M., Nieuwland, G. and Meesters, E. H.: Coral Growth Rates Revisited after 31 Years: What is Causing
560 Lower Extension Rates in Acropora Palmata?, Bull. Mar. Sci., 84(3), 287–294, 2009.

561 Bannerot, S. P. and Bohnsack, J. A.: A stationary visual census technique for quantitatively assessing community
562 structure of coral reef fishes, NOAA. [online] Available from: http://core.kmi.open.ac.uk/download/pdf/11018492.pdf
563 (Accessed 1 September 2014), 1986.

564 Bates, N. R., Amat, A. and Andersson, A. J.: Feedbacks and responses of coral calcification on the Bermuda reef
565 system to seasonal changes in biological processes and ocean acidification, Biogeosciences, 7(8), 2509–2530,
566 doi:10.5194/bg-7-2509-2010, 2010.

567 Bednarz, V., Cardini, U., van Hoytema, N., Al-Rshaidat, M. and Wild, C.: Seasonal variation in dinitrogen fixation
568 and oxygen fluxes associated with two dominant zooxanthellate soft corals from the northern Red Sea, Mar. Ecol.
569 Prog. Ser., 519, 141–152, doi:10.3354/meps11091, 2015.

570 Bellwood, D. R.: Direct estimate of bioerosion by two parrotfish species, Chlorurus gibbus and C. sordidus, on the
571 Great Barrier Reef, Australia, Mar. Biol., 121(3), 419–429, doi:10.1007/BF00349451, 1995.

572 Bockmon, E. E. and Dickson, A. G.: An inter-laboratory comparison assessing the quality of seawater carbon dioxide
573 measurements, Mar. Chem., 171, 36–43, doi:10.1016/j.marchem.2015.02.002, 2015.

574 Bronstein, O. and Loya, Y.: Echinoid community structure and rates of herbivory and bioerosion on exposed and
575 sheltered reefs, J. Exp. Mar. Biol. Ecol., 456, 8–17, doi:10.1016/j.jembe.2014.03.003, 2014.

576 Browne, N. K., Smithers, S. G. and Perry, C. T.: Carbonate and terrigenous sediment budgets for two inshore turbid
577 reefs on the central Great Barrier Reef, Mar. Geol., 346, 101–123, doi:10.1016/j.margeo.2013.08.011, 2013.

578 Bruggemann, J., van Kessel, A., van Rooij, J. and Breeman, A.: Bioerosion and sediment ingestion by the Caribbean
579 parrotfish Scarus vetula and Sparisoma viride: implications of fish size, feeding mode and habitat use, Mar. Ecol.
580 Prog. Ser., 134, 59–71, doi:10.3354/meps134059, 1996.

581 Buddemeier, R. W.: Symbiosis: Making light work of adaptation, Nature, 388(6639), 229–230, doi:10.1038/40755,
582 1997.

583 Cai, W.-J., Ma, Y., Hopkinson, B. M., Grottoli, A. G., Warner, M. E., Ding, Q., Hu, X., Yuan, X., Schoepf, V., Xu,
584 H., Han, C., Melman, T. F., Hoadley, K. D., Pettay, D. T., Matsui, Y., Baumann, J. H., Levas, S., Ying, Y. and Wang,
585 Y.: Microelectrode characterization of coral daytime interior pH and carbonate chemistry, Nat. Commun., 7, 11144,
586 doi:10.1038/ncomms11144, 2016.

587 Camp, E. F., Nitschke, M. R., Rodolfo-Metalpa, R., Houlbreque, F., Gardner, S. G., Smith, D. J., Zampighi, M. and
588 Suggett, D. J.: Reef-building corals thrive within hot-acidified and deoxygenated waters, Sci. Rep., 7(1), 2434,
589 doi:10.1038/s41598-017-02383-y, 2017.

590 Camp, E. F., Schoepf, V., Mumby, P. J., Hardtke, L. A., Rodolfo-Metalpa, R., Smith, D. J. and Suggett, D. J.: The
591 Future of Coral Reefs Subject to Rapid Climate Change: Lessons from Natural Extreme Environments, Front. Mar.
592 Sci., 5, doi:10.3389/fmars.2018.00004, 2018.

593 Cantin, N. E., Cohen, A. L., Karnauskas, K. B., Tarrant, A. M. and McCorkle, D. C.: Ocean Warming Slows Coral
594 Growth in the Central Red Sea, Science, 329(5989), 322–325, doi:10.1126/science.1190182, 2010.

595 Carricart-Ganivet, J. P., Cabanillas-Terán, N., Cruz-Ortega, I. and Blanchon, P.: Sensitivity of Calcification to
596 Thermal Stress Varies among Genera of Massive Reef-Building Corals, PLoS ONE, 7(3), e32859,
597 doi:10.1371/journal.pone.0032859, 2012.

598 Chazottes, V., Le Campion-Alsumard, T., Peyrot-Clausade, M. and Cuet, P.: The effects of eutrophication-related
599 alterations to coral reef communities on agents and rates of bioerosion (Reunion Island, Indian Ocean), Coral Reefs,
600 21(4), 375–390, 2002.

601 Cohen, A. L. and Holcomb, M.: Why corals care about ocean acidification: uncovering the mechanism, Oceanography,
602 (22), 118–127, 2009.

603 Cooper, T. F., Death, G., Fabricius, K. E. and Lough, J. M.: Declining coral calcification in massive Porites in two
604 nearshore regions of the northern Great Barrier Reef, Glob. Change Biol., 14(3), 529–538, doi:10.1111/j.1365-
605 2486.2007.01520.x, 2008.

606 Couce, E., Ridgwell, A. and Hendy, E. J.: Environmental controls on the global distribution of shallow-water coral
607 reefs, J. Biogeogr., 39(8), 1508–1523, doi:10.1111/j.1365-2699.2012.02706.x, 2012.

608 Cyronak, T., Schulz, K. G., Santos, I. R. and Eyre, B. D.: Enhanced acidification of global coral reefs driven by
609 regional biogeochemical feedbacks, Geophys. Res. Lett., 2014GL060849, doi:10.1002/2014GL060849, 2014.

610 Death, G., Lough, J. M. and Fabricius, K. E.: Declining Coral Calcification on the Great Barrier Reef, Science,
611 323(5910), 116–119, doi:10.1126/science.1165283, 2009.

612 Dullo, W.-C., Reijmer, J., Schuhmacher, H., Eisenhauer, A., Hassan, M. and Heiss, G.: Holocene reef growth and
613 recent carbonate production in the Red Sea, [online] Available from:
614 https://www.researchgate.net/publication/230751439_Holocene_reef_growth_and_recent_carbonate_production_in
615 _the_Red_Sea, 1996.

616 Eakin, C. M.: A tale of two Enso Events: carbonate budgets and the influence of two warming disturbances and
617 intervening variability, Uva Island, Panama, Bull. Mar. Sci., 69(1), 171–186, 2001.

618 Edgar, G. J., Banks, S. A., Brandt, M., Bustamante, R. H., Chiriboga, A., Earle, S. A., Garske, L. E., Glynn, P. W.,
619 Grove, J. S., Henderson, S., Hickman, C. P., Miller, K. A., Rivera, F. and Wellington, G. M.: El Niño, grazers and
620 fisheries interact to greatly elevate extinction risk for Galapagos marine species, Glob. Change Biol., 16(10), 2876–
621 2890, doi:10.1111/j.1365-2486.2009.02117.x, 2010.

622 Edinger, E. N., Limmon, G. V., Jompa, J., Widjatmoko, W., Heikoop, J. M. and Risk, M. J.: Normal coral growth
623 rates on dying reefs: Are coral growth rates good indicators of reef health?, Mar. Pollut. Bull., 40(5), 404–425, 2000.

624 Enochs, I. C.: Ocean acidification enhances the bioerosion of a common coral reef sponge: implications for the
625 persistence of the Florida Reef Tract, Bull. Mar. Sci., 91, 271–290, doi:10.5343/bms.2014.1045, 2015.

626 Ezzat, L., Maguer, J.-F., Grover, R. and Ferrier-Pagès, C.: Limited phosphorus availability is the Achilles heel of
627 tropical reef corals in a warming ocean, Sci. Rep., 6, 31768, doi:10.1038/srep31768, 2016.

628 Fabricius, K. E.: Effects of terrestrial runoff on the ecology of corals and coral reefs: review and synthesis, Mar. Pollut.
629 Bull., 50(2), 125–146, doi:10.1016/j.marpolbul.2004.11.028, 2005.

630 Fang, J. K. H., Mello-Athayde, M. A., Schönberg, C. H. L., Kline, D. I., Hoegh-Guldberg, O. and Dove, S.: Sponge
631 biomass and bioerosion rates increase under ocean warming and acidification, Glob. Change Biol., 19(12), 3581–
632 3591, doi:10.1111/gcb.12334, 2013.

633 Ferrier-Pagès, C., Godinot, C., D'Angelo, C., Wiedenmann, J. and Grover, R.: Phosphorus metabolism of reef
634 organisms with algal symbionts, Ecol. Monogr., 86(3), 262–277, doi:10.1002/ecm.1217, 2016.

635 Franco, C., Hepburn, L. A., Smith, D. J., Nimrod, S. and Tucker, A.: A Bayesian Belief Network to assess rate of
636 changes in coral reef ecosystems, Environ. Model. Softw., 80, 132–142, doi:10.1016/j.envsoft.2016.02.029, 2016.

637 Glynn, P. W.: Bioerosion and coral-reef growth: a dynamic balance, in Life and Death of Coral Reefs, edited by C.
638 Birkeland, pp. 68–94, Chapman and Hall, Ney York, USA., 1997.

639 Glynn, P. W. and Manzello, D. P.: Bioerosion and Coral Reef Growth: A Dynamic Balance, in Coral Reefs in the
640 Anthropocene, edited by C. Birkeland, pp. 67–97, Springer Netherlands., 2015.

641 Gray, S. E. C., DeGrandpre, M. D., Langdon, C. and Corredor, J. E.: Short-term and seasonal pH, pCO2 and saturation
642 state variability in a coral-reef ecosystem, Glob. Biogeochem. Cycles, 26(3), doi:10.1029/2011GB004114, 2012.

643 Green, A. L. and Bellwood, D. R.: Monitoring functional groups of herbivorous reef fishes as indicators of coral reef
644 resilience: a practical guide for coral reef managers in the Asia Pacific region, International Union for Conservation
645 of Nature, IUCN, Gland, Switzerland. [online] Available from:
646 ftp://ftp.library.noaa.gov/noaa_documents.lib/CoRIS/IUCN_herbivorous_reef-fishes_2009.pdf (Accessed 30
647 September 2017), 2009.

648 Heiss, G. A.: Carbonate production by scleractinian corals at Aqaba, Gulf of Aqaba, Red Sea, Facies, 33(1), 19–34,
649 doi:10.1007/BF02537443, 1995.

650 Hoey, A. S. and Bellwood, D. R.: Cross-shelf variation in the role of parrotfishes on the Great Barrier Reef, Coral
651 Reefs, 27(1), 37–47, doi:10.1007/s00338-007-0287-x, 2007.

652 Hofmann, G. E., Smith, J. E., Johnson, K. S., Send, U., Levin, L. A., Micheli, F., Paytan, A., Price, N. N., Peterson,
653 B., Takeshita, Y., Matson, P. G., Crook, E. D., Kroeker, K. J., Gambi, M. C., Rivest, E. B., Frieder, C. A., Yu, P. C.
654 and Martz, T. R.: High-Frequency Dynamics of Ocean pH: A Multi-Ecosystem Comparison, edited by W.-C. Chin,
655 PLoS ONE, 6(12), e28983, doi:10.1371/journal.pone.0028983, 2011.

656 Jokiel, P. L. and Coles, S. L.: Response of Hawaiian and other Indo-Pacific reef corals to elevated temperature, Coral
657 Reefs, 8(4), 155–162, doi:10.1007/BF00265006, 1990.

658 Jones, N. S., Ridgwell, A. and Hendy, E. J.: Evaluation of coral reef carbonate production models at a global scale,
659 Biogeosciences, 12(5), 1339–1356, doi:10.5194/bg-12-1339-2015, 2015.

660 Kattan, A., Coker, D. J. and Berumen, M. L.: Reef fish communities in the central Red Sea show evidence of
661 asymmetrical fishing pressure, Mar. Biodivers., 1–12, doi:10.1007/s12526-017-0665-8, 2017.

662 Kennedy, E. V., Perry, C. T., Halloran, P. R., Iglesias-Prieto, R., Schönberg, C. H. L., Wisshak, M., Form, A. U.,
663 Carricart-Ganivet, J. P., Fine, M., Eakin, C. M. and Mumby, P. J.: Avoiding Coral Reef Functional Collapse Requires
664 Local and Global Action, Curr. Biol., 23(10), 912–918, doi:10.1016/j.cub.2013.04.020, 2013.

665 Kleypas, J., Buddemeier, R. and Gattuso, J.-P.: The future of coral reefs in an age of global change, Int. J. Earth Sci.,
666 90(2), 426–437, doi:10.1007/s005310000125, 2001.

667 Kleypas, J. A., McManus, J. W. and Menez, L. A. B.: Environmental Limits to Coral Reef Development: Where Do
668 We Draw the Line?, Am. Zool., 39, 146–159, 1999.

669 Mallela, J. and Perry, C.: Calcium carbonate budgets for two coral reefs affected by different terrestrial runoff regimes,
670 Rio Bueno, Jamaica, Coral Reefs, 26(1), 129–145, doi:10.1007/s00338-006-0169-7, 2007.

671 Manzello, D. P.: Ocean acidification hotspots: Spatiotemporal dynamics of the seawater CO2 system of eastern Pacific
672 coral reefs, Limnol. Oceanogr., 55(1), 239–248, doi:10.4319/lo.2010.55.1.0239, 2010.

673 Manzello, D. P., Kleypas, J. A., Budd, D. A., Eakin, C. M., Glynn, P. W. and Langdon, C.: Poorly cemented coral
674 reefs of the eastern tropical Pacific: Possible insights into reef development in a high-CO2 world, Proc. Natl. Acad.
675 Sci., 105(30), 10450–10455, 2008.

676 Marshall, A. T. and Clode, P.: Calcification rate and the effect of temperature in a zooxanthellate and an
677 azooxanthellate scleractinian reef coral, Coral Reefs, 23(2), 218–224, doi:10.1007/s00338-004-0369-y, 2004.

678 Marubini, F., Ferrier-Pagès, C., Furla, P. and Allemand, D.: Coral calcification responds to seawater acidification: a
679 working hypothesis towards a physiological mechanism, Coral Reefs, 27(3), 491–499, doi:10.1007/s00338-008-0375-
680 6, 2008.

681 McClanahan, T. R.: Kenyan coral reef lagoon fish: effects of fishing, substrate complexity, and sea urchins, Coral
682 Reefs, 13(4), 231–241, doi:10.1007/BF00303637, 1994.

683 McClanahan, T. R. and Shafir, S. H.: Causes and consequences of sea urchin abundance and diversity in Kenyan coral
684 reef lagoons, Oecologia, 83(3), 362–370, doi:10.1007/BF00317561, 1990.

685 McClanahan, T. R., Nugues, M. and Mwachireya, S.: Fish and sea urchin herbivory and competition in Kenyan coral
686 reef lagoons: the role of reef management, J. Exp. Mar. Biol. Ecol., 184(2), 237–254, doi:10.1016/0022-
687 0981(94)90007-8, 1994.

688 Metzl, N., Moore, B., Papaud, A. and Poisson, A.: Transport and carbon exchanges in Red Sea Inverse Methodology,
689 Glob. Biogeochem. Cycles, 3(1), 1–26, doi:10.1029/GB003i001p00001, 1989.

690 Moberg, F. and Folke, C.: Ecological goods and services of coral reef ecosystems, Ecol. Econ., 29, 215–233, 1999.

691 Monroe, A. A., Ziegler, M., Roik, A., Röthig, T., Hardenstin, R., Emms, M., Jensen, T., Voolstra, C. R. and Berumen,
692 M. L.: In situ observations of coral bleaching in the central Saudi Arabian Red Sea during the 2015/2016 global coral
693 bleaching event, PloS ONE, accepted.

694 Mumby, P. J.: The Impact Of Exploiting Grazers (Scaridae) On The Dynamics Of Caribbean Coral Reefs, Ecol. Appl.,
695 16(2), 747–769, doi:10.1890/1051-0761(2006)016[0747:TIOEGS]2.0.CO;2, 2006.

696 Orr, J. C., Fabry, V. J., Aumont, O., Bopp, L., Doney, S. C., Feely, R. A., Gnanadesikan, A., Gruber, N., Ishida, A.,
697 Joos, F., Key, R. M., Lindsay, K., Maier-Reimer, E., Matear, R., Monfray, P., Mouchet, A., Najjar, R. G., Plattner,
698 G.-K., Rodgers, K. B., Sabine, C. L., Sarmiento, J. L., Schlitzer, R., Slater, R. D., Totterdell, I. J., Weirig, M.-F.,
699 Yamanaka, Y. and Yool, A.: Anthropogenic ocean acidification over the twenty-first century and its impact on
700 calcifying organisms, Nature, 437(7059), 681–686, doi:10.1038/nature04095, 2005.

701 Page, H. N., Andersson, A. J., Jokiel, P. L., Rodgers, K. S., Lebrato, M., Yeakel, K., Davidson, C., D'Angelo, S. and
702 Bahr, K. D.: Differential modification of seawater carbonate chemistry by major coral reef benthic communities, Coral
703 Reefs, 1–15, doi:10.1007/s00338-016-1490-4, 2016.

704 Pari, N., Peyrot-Clausade, M., Le Champion-Alsumard, T., Hutchings, P., Chazottes, V., Gobulic, S., Le Champion,
705 J. and Fontaine, M. F.: Bioerosion of experimental substrates on high islands and on atoll lagoons (French Polynesia)
706 after two years of exposure, Mar. Ecol. Prog. Ser., 166, 119–130, 1998.

707 Perry, C., Edinger, E., Kench, P., Murphy, G., Smithers, S., Steneck, R. and Mumby, P.: Estimating rates of
708 biologically driven coral reef framework production and erosion: a new census-based carbonate budget methodology
709 and applications to the reefs of Bonaire, Coral Reefs, 31(3), 853–868, doi:10.1007/s00338-012-0901-4, 2012.

710 Perry, C. T., Spencer, T. and Kench, P. S.: Carbonate budgets and reef production states: a geomorphic perspective
711 on the ecological phase-shift concept, Coral Reefs, 27(4), 853–866, doi:10.1007/s00338-008-0418-z, 2008.

712 Perry, C. T., Murphy, G. N., Kench, P. S., Smithers, S. G., Edinger, E. N., Steneck, R. S. and Mumby, P. J.: Caribbean-
713 wide decline in carbonate production threatens coral reef growth, Nat. Commun., 4, 1402, doi:10.1038/ncomms2409,
714 2013.

715 Perry, C. T., Murphy, G. N., Kench, P. S., Edinger, E. N., Smithers, S. G., Steneck, R. S. and Mumby, P. J.: Changing
716 dynamics of Caribbean reef carbonate budgets: emergence of reef bioeroders as critical controls on present and future
717 reef growth potential, Proc. R. Soc. B Biol. Sci., 281(1796), 20142018–20142018, doi:10.1098/rspb.2014.2018, 2014.

718 Perry, C. T., Murphy, G. N., Graham, N. A. J., Wilson, S. K., Januchowski-Hartley, F. A. and East, H. K.: Remote
719 coral reefs can sustain high growth potential and may match future sea-level trends, Sci. Rep., 5, 18289,
720 doi:10.1038/srep18289, 2015.

721 Pogoreutz, C., Rädecker, N., Cárdenas, A., Gärdes, A., Voolstra, C. R. and Wild, C.: Sugar enrichment provides
722 evidence for a role of nitrogen fixation in coral bleaching, Glob. Change Biol., 8, 23:3838–3848,
723 doi:10.1111/gcb.13695, 2017.

724 R Core Team: R: A language and environment for statistical computing, R Foundation for Statistical Computing,
725 Vienna, Austria. [online] Available from: http://www.R-project.org/, 2013.

726 Rädecker, N., Pogoreutz, C., Voolstra, C. R., Wiedenmann, J. and Wild, C.: Nitrogen cycling in corals: the key to
727 understanding holobiont functioning?, Trends Microbiol., doi:10.1016/j.tim.2015.03.008, 2015.

728 Raitsos, D. E., Hoteit, I., Prihartato, P. K., Chronis, T., Triantafyllou, G. and Abualnaja, Y.: Abrupt warming of the
729 Red Sea, Geophys. Res. Lett., 38(14), L14601, doi:10.1029/2011GL047984, 2011.

730 Raitsos, D. E., Pradhan, Y., Brewin, R. J. W., Stenchikov, G. and Hoteit, I.: Remote Sensing the Phytoplankton
731 Seasonal Succession of the Red Sea, PLoS ONE, 8(6), e64909, doi:10.1371/journal.pone.0064909, 2013.

732 Reaka-Kudla, M. L.: The Global Biodiversity of Coral Reefs: A Comparison with Rainforests, in Biodiversity II:
733 Understanding and Protecting Our Biological Resources, edited by M. L. Reaka-Kudla, D. E. Wilson, and E. O.
734 Wilson, pp. 83–106, The Joseph Henry Press, USA., 1997.

735 Riegl, B.: Climate change and coral reefs: different effects in two high-latitude areas (Arabian Gulf, South Africa),
736 Coral Reefs, 22(4), 433–446, doi:10.1007/s00338-003-0335-0, 2003.

737 Riegl, B. M., Bruckner, A. W., Rowlands, G. P., Purkis, S. J. and Renaud, P.: Red Sea Coral Reef Trajectories over 2
738 Decades Suggest Increasing Community Homogenization and Decline in Coral Size, PLoS ONE, 7(5), e38396,
739 doi:10.1371/journal.pone.0038396, 2012.

740 Roik, A., Roder, C., Röthig, T. and Voolstra, C. R.: Spatial and seasonal reef calcification in corals and calcareous
741 crusts in the central Red Sea, Coral Reefs, 1–13, doi:10.1007/s00338-015-1383-y, 2015.

742 Roik, A., Röthig, T., Roder, C., Ziegler, M., Kremb, S. G. and Voolstra, C. R.: Year-Long Monitoring of Physico-
743 Chemical and Biological Variables Provide a Comparative Baseline of Coral Reef Functioning in the Central Red Sea,
744 PLOS ONE, 11(11), e0163939, doi:10.1371/journal. pone.0163939, 2016.

745 Sawall, Y. and Al-Sofyani, A.: Biology of Red Sea Corals: Metabolism, Reproduction, Acclimatization, and
746 Adaptation, in The Red Sea, edited by N. M. A. Rasul and I. C. F. Stewart, pp. 487–509, Springer Berlin Heidelberg.
747 [online] Available from: http://link.springer.com/chapter/10.1007/978-3-662-45201-1_28 (Accessed 7 April 2015),
748 2015.

749 Sawall, Y., Al-Sofyani, A., Hohn, S., Banguera-Hinestroza, E., Voolstra, C. R. and Wahl, M.: Extensive phenotypic
750 plasticity of a Red Sea coral over a strong latitudinal temperature gradient suggests limited acclimatization potential
751 to warming, Sci. Rep., 5, 8940, doi:10.1038/srep08940, 2015.

752 Schmidt, G. M. and Richter, C.: Coral Growth and Bioerosion of Porites lutea in Response to Large Amplitude Internal
753 Waves, PLoS ONE, 8(12), e73236, doi:10.1371/journal.pone.0073236, 2013.

754 Schneider, K. and Erez, J.: The effect of carbonate chemistry on calcification and photosynthesis in the hermatypic
755 coral Acropora eurystoma, Limnol. Oceanogr., 51(3), 1284–1293, 2006.

756 Schuhmacher, H., Loch, K., Loch, W. and See, W. R.: The aftermath of coral bleaching on a Maldivian reef—a
757 quantitative study, Facies, 51(1–4), 80–92, doi:10.1007/s10347-005-0020-6, 2005.

758 Sheppard, C. and Loughland, R.: Coral mortality and recovery in response to increasing temperature in the southern
759 Arabian Gulf, Aquat. Ecosyst. Health Manag., 5(4), 395–402, doi:10.1080/14634980290002020, 2002.

760 Silbiger, N. J., Guadayol, O., Thomas, F. I. M. and Donahue, M. J.: Reefs shift from net accretion to net erosion along
761 a natural environmental gradient, Mar. Ecol. Prog. Ser., 515, 33–44, doi:10.3354/meps10999, 2014.

762 Silverman, J., Lazar, B. and Erez, J.: Community metabolism of a coral reef exposed to naturally varying dissolved
763 inorganic nutrient loads, Biogeochemistry, 84(1), 67–82, doi:10.1007/s10533-007-9075-5, 2007.

764 Steiner, Z., Erez, J., Shemesh, A., Yam, R., Katz, A. and Lazar, B.: Basin-scale estimates of pelagic and coral reef
765 calcification in the Red Sea and Western Indian Ocean, Proc. Natl. Acad. Sci., 1414323111,
766 doi:10.1073/pnas.1414323111, 2014.

767 Tambutté, S., Holcomb, M., Ferrier-Pagès, C., Reynaud, S., Tambutté, É., Zoccola, D. and Allemand, D.: Coral
768 biomineralization: From the gene to the environment, J. Exp. Mar. Biol. Ecol., 408(1–2), 58–78,
769 doi:10.1016/j.jembe.2011.07.026, 2011.

770 Tribollet, A., Decherf, G., Hutchings, P. and Peyrot-Clausade, M.: Large-scale spatial variability in bioerosion of
771 experimental coral substrates on the Great Barrier Reef (Australia): importance of microborers, Coral Reefs, 21(4),
772 424–432, doi:10.1007/s00338-002-0267-0, 2002.

773 Tribollet, A., Godinot, C., Atkinson, M. and Langdon, C.: Effects of elevated pCO2 on dissolution of coral carbonates
774 by microbial euendoliths, Glob. Biogeochem. Cycles, 23(3), doi:10.1029/2008GB003286, 2009.

775 Uthicke, S., Furnas, M. and Lønborg, C.: Coral Reefs on the Edge? Carbon Chemistry on Inshore Reefs of the Great
776 Barrier Reef, PLoS ONE, 9(10), e109092, doi:10.1371/journal.pone.0109092, 2014.

777 Waldbusser, G. G., Hales, B. and Haley, B. A.: Calcium carbonate saturation state: on myths and this or that stories,
778 ICES J. Mar. Sci. J. Cons., 73(3), 563–568, doi:10.1093/icesjms/fsv174, 2016.

779 Wickham, H. and Chang, W.: ggplot2: An Implementation of the Grammar of Graphics. [online] Available from:
780 http://cran.r-project.org/web/packages/ggplot2/index.html (Accessed 25 June 2015), 2015.

781 Wiedenmann, J., D'Angelo, C., Smith, E. G., Hunt, A. N., Legiret, F.-E., Postle, A. D. and Achterberg, E. P.: Nutrient
782 enrichment can increase the susceptibility of reef corals to bleaching, Nat. Clim. Change, 3(2), 160–164,
783 doi:10.1038/nclimate1661, 2013.

784 Yeakel, K. L., Andersson, A. J., Bates, N. R., Noyes, T. J., Collins, A. and Garley, R.: Shifts in coral reef
785 biogeochemistry and resulting acidification linked to offshore productivity, Proc. Natl. Acad. Sci., 112(47), 14512–
786 14517, doi:10.1073/pnas.1507021112, 2015.

787 Zaneveld, J. R., Burkepile, D. E., Shantz, A. A., Pritchard, C. E., McMinds, R., Payet, J. P., Welsh, R., Correa, A. M.
788 S., Lemoine, N. P., Rosales, S., Fuchs, C., Maynard, J. A. and Thurber, R. V.: Overfishing and nutrient pollution
789 interact with temperature to disrupt coral reefs down to microbial scales, Nat. Commun., 7, 11833,
790 doi:10.1038/ncomms11833, 2016.

791 Zundelevich, A., Lazar, B. and Ilan, M.: Chemical versus mechanical bioerosion of coral reefs by boring sponges -
792 lessons from Pione cf. vastifica, J. Exp. Biol., 210(1), 91–96, doi:10.1242/jeb.02627, 2007.

793

794 **Figures**

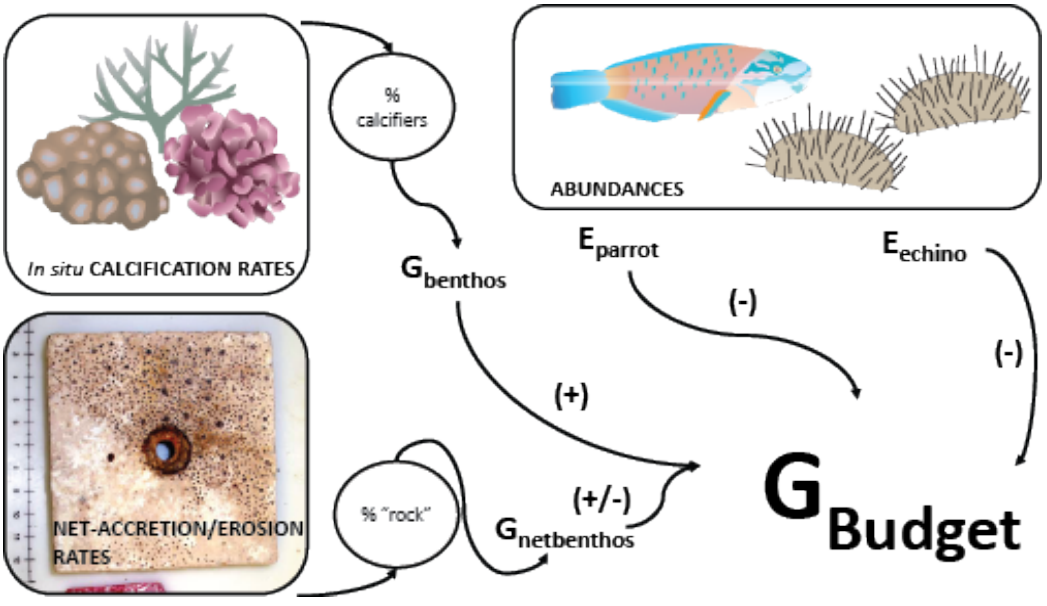

795

796 **Figure 1. Schematic overview of the census based *ReefBudget* carbonate budget (G_{budget}) approach (adapted from Perry et**
797 **al., 2012).** Values and equations that were used are available as Supplementary Materials. $G_{benthos}$ = benthic community calcification
798 rate, $G_{netbenthos}$ = net-accretion/erosion rate of bare reef substrate, E_{parrot} = parrotfish erosion rate, E_{echino} = echinoid (sea urchin)
799 erosion rate, G_{budget} = carbonate budget of a reef. Images from *www.ian.umces.edu*.

Biogeosciences Discuss., https://doi.org/10.5194/bg-2018-57
Manuscript under review for journal Biogeosciences
Discussion started: 28 February 2018

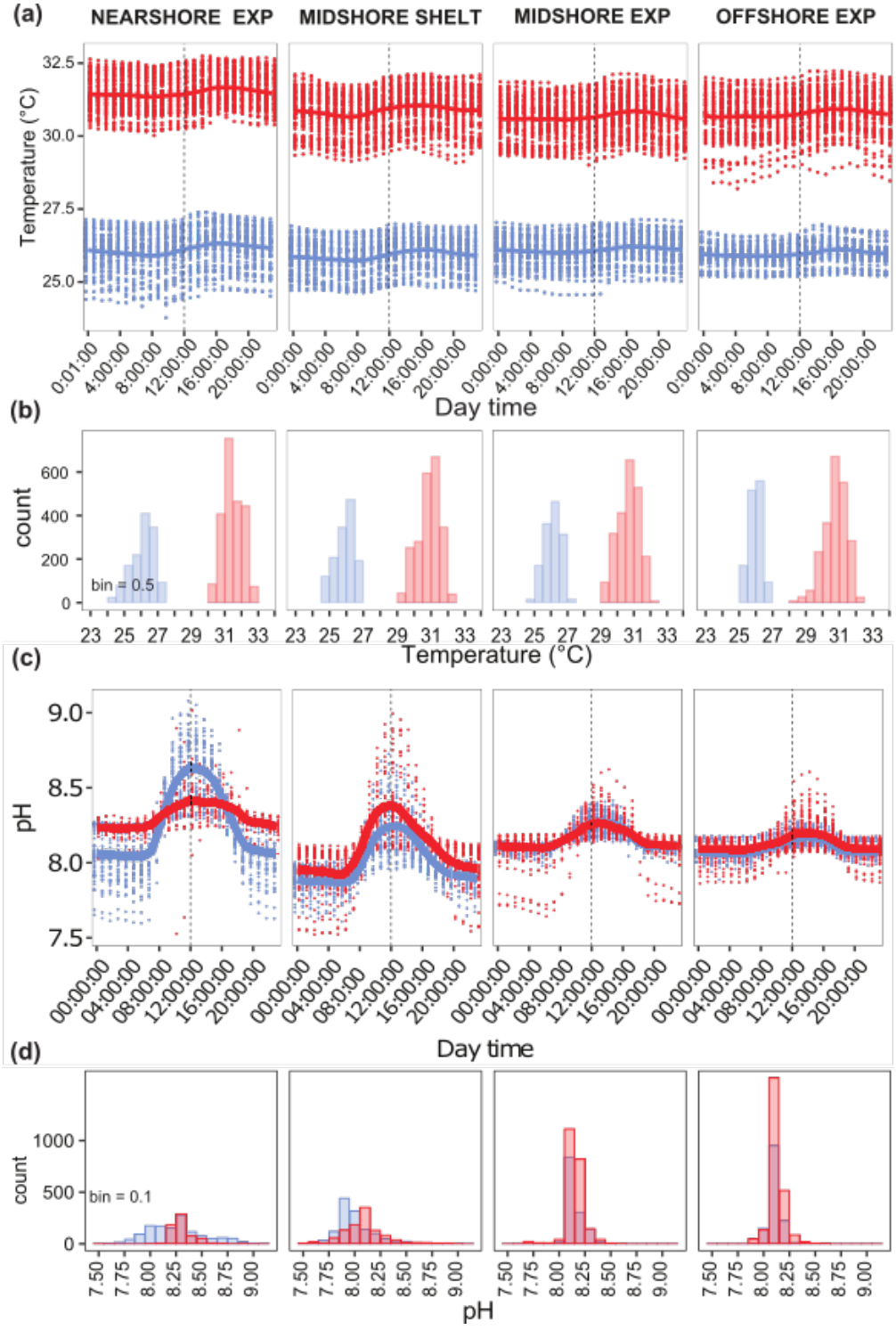

Biogeosciences Discuss., https://doi.org/10.5194/bg-2018-57
Manuscript under review for journal Biogeosciences
Discussion started: 28 February 2018

801 **Figure 2. Seasonal temperature and pH regimes on coral reefs along a cross-shelf gradient in the central Red Sea.** Continuous
802 temperatures (a)-(b) and $pH_{(continuous)}$ (c)-(d) collected during winter (blue) and summer (red) at 0.5 m above the reef are presented
803 as diel profiles (a), (c) and in histograms (b), (d). Data points per reef site in winter comprise n = 1287 - 1344, and n = 1099 - 2231
804 in summer (nearshore summer n = 644). Diel profiles show raw data points and local polynomial regression lines (LOESS, span =
805 0.1). A dotted vertical line marks the midday time. EXP = exposed, SHELT = sheltered.

806

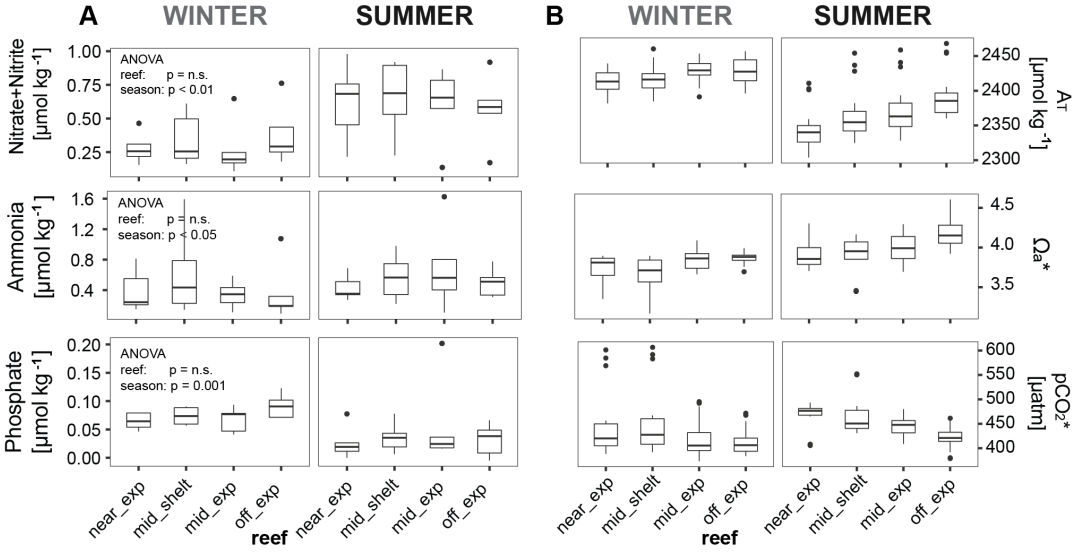

807

808 **Figure 3. Inorganic nutrients and carbonate system conditions across reef sites and seasons in the central Red Sea.** Boxplots
809 illustrate the differences of seawater parameters (measured and *estimated) between the reefs within each season (box: 1st and 3rd
810 quartiles, whiskers: 1.5-fold inter-quartile range, points: data beyond this range). A_T = total alkalinity, Ω_a = aragonite saturation
811 state, pCO_2 = carbon dioxide; off = offshore, mid = midshore, near = nearshore, exp = exposed forereef, shelt = sheltered lagoon,
812 n.s. = not significant.
813

Biogeosciences Discuss., https://doi.org/10.5194/bg-2018-57
Manuscript under review for journal Biogeosciences
Discussion started: 28 February 2018

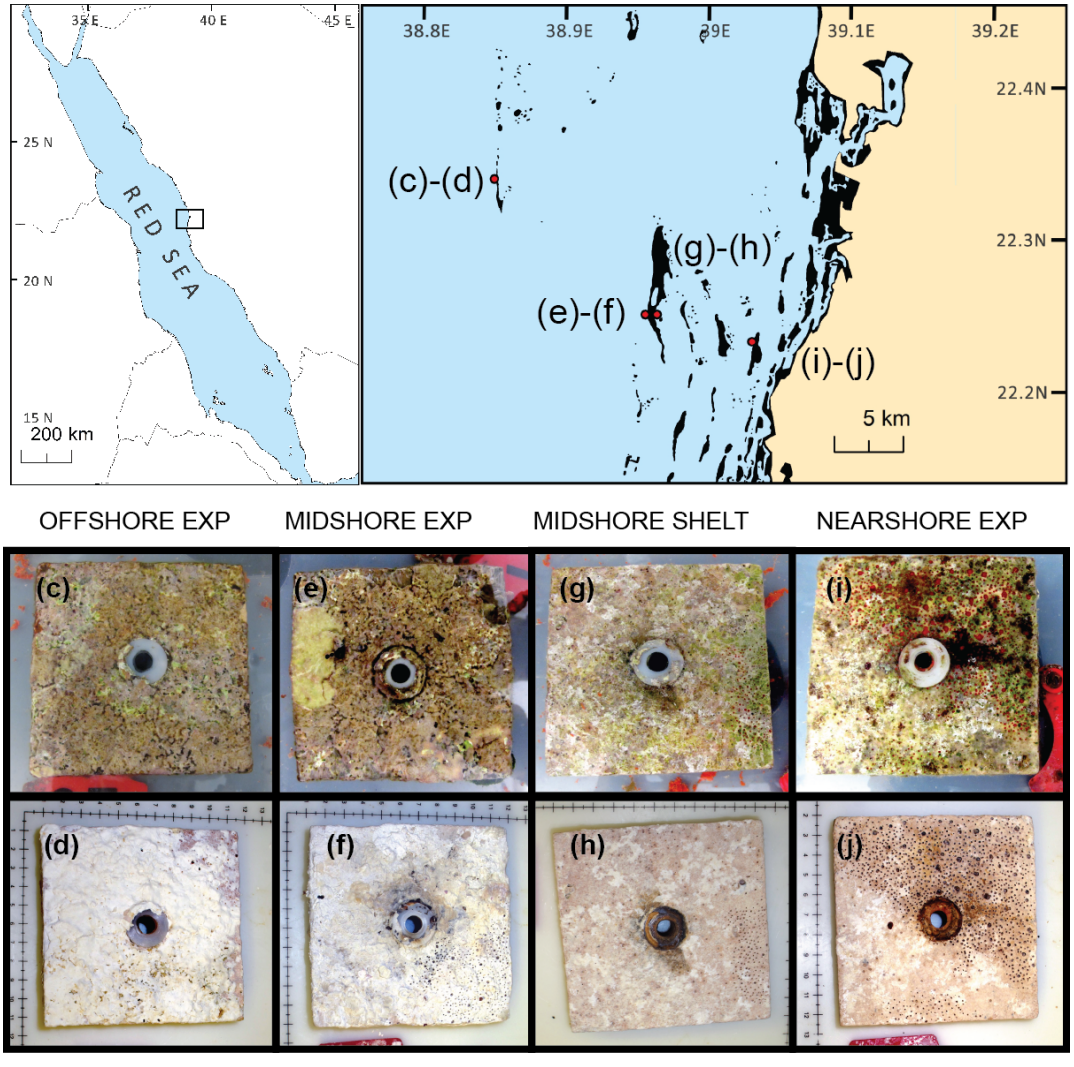

Figure 4. Study sites and limestone blocks (100 x 100 mm) after 30 months of deployment in the reef sites for measurements of net-accretion/erosion rates G_{net}. Maps of the central Red Sea (a)-(b) indicate the study sites along a cross-shelf gradient. Photos (c), (e), (g), and (f) show freshly collected limestone blocks that were recovered after 30 months, and in photos (d), (f), (h), and (j) the same blocks after bleaching and drying are presented. Boring holes of endolithic sponges are clearly visible in the nearshore exposed and both midshore reef sites. In the midshore and offshore exposed reefs, blocks were covered with crusts of biogenic carbonate mostly accreted by coralline algae assemblages. EXP = exposed, SHELT = sheltered, scales in the photos show cm. Also see Fig. S1 of the Supplementary Material for an illustration of the data from the limestone block "assay". (Map has been adapted from Roik et al. (2015); map credits: Maha Khalil).

Biogeosciences Discuss., https://doi.org/10.5194/bg-2018-57
Manuscript under review for journal Biogeosciences
Discussion started: 28 February 2018

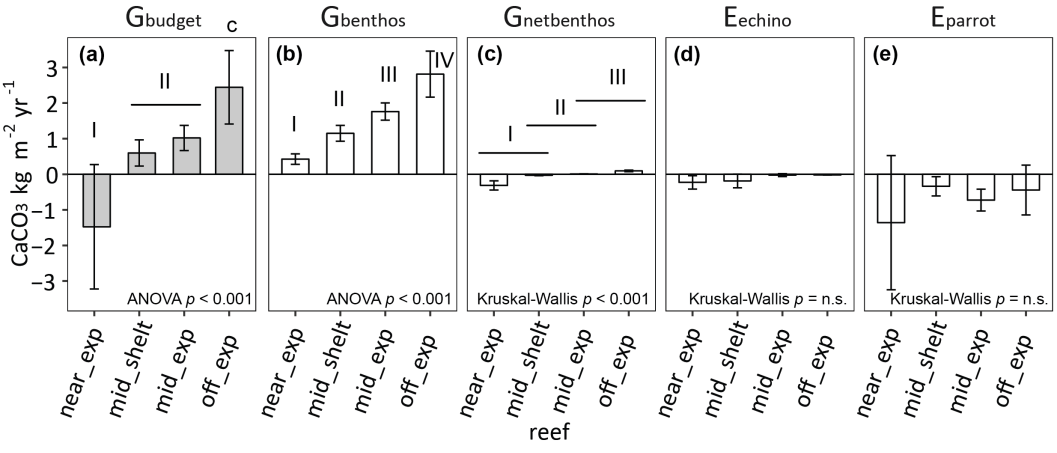

Figure 5. Reef carbonate budget estimates and contributing biotic variables along a cross-shelf gradient in the central Red Sea. Benthos accretion ($G_{benthos}$, $G_{netbenthos}$), and the erosion rates of echinoids and parrotfishes (E_{echino}, E_{parrot}) contribute to the total reef carbonate budget (G_{budget}) at each reef site. All data are presented as mean ± standard deviation. (a) G_{budget} and (b)-(e) biotic variables ($G_{benthos}$, $G_{netbenthos}$, E_{echino}, E_{parrot}). (I-IV) indicate significant differences between the sites. Near_exp = nearshore exposed, mid_shelt = midshore sheltered (lagoon), mid_exp = midshore exposed, off_exp = offshore exposed.

Biogeosciences Discuss., https://doi.org/10.5194/bg-2018-57
Manuscript under review for journal Biogeosciences
Discussion started: 28 February 2018

834 **Tables**

835 **Table 1. Abiotic parameters relevant for reef growth at coral reef sites along a cross-shelf gradient in the central Red Sea.** Temperature (Temp) and
836 $pH_{(continuous)}$ were continuously measured using *in situ* probes (CTDs). Weekly collected seawater samples were used for the determination of inorganic nutrient
837 concentrations, i.e. nitrate and nitrite (NO_3^-&NO_2^-), ammonia (NH_4^+), and phosphate (PO_4^{3-}). Carbonate chemistry parameters were measured as A_T and $pH_{(discrete)}$
838 in the same samples and used to estimate (*) the carbonate ion concentration (CO_3^{2-}), aragonite saturation state (Ω_a), total inorganic carbon (C_T), bicarbonate ion
839 (HCO_3^-), and partial pressure of carbon dioxide (pCO_2). Mean (standard deviation).

	Continuous data						Seawater samples					
Site / Season	**Temp**	**pH (contin.)**	**NO_3^- &NO_2^-**	**NH_4^+**	**PO_4^{3-}**	**pH (discrete)**	**A_T**	**HCO_3^{-*}**	**CO_3^{2-*}**	**Ωa^***	**C_T^***	**pCO_2***
	°C		**µmol kg^{-1}**	**µmol kg^{-1}**	**µmol kg^{-1}**		**µmol kg^{-1}**	**µmol kg^{-1}**	**µmol kg^{-1}**		**µmol kg^{-1}**	**µatm**
Avg. winter	26.0 (0.6)	8.13 (0.19)	0.32 (0.18)	0.44 (0.37)	0.07 (0.02)	8.140 (0.041)	2422 (20)	1821 (31)	244 (13)	3.77 (0.19)	2076 (23)	436 (59)
Avg. summer	31.0 (0.7)	8.15 (0.19)	0.61 (0.24)	0.54 (0.30)	0.04 (0.04)	8.127 (0.029)	2369 (38)	1740 (37)	254 (14)	4.00 (0.23)	2005 (36)	451 (34)
Nearshore exposed / winter	26.1 (0.7)	8.25 (0.27)	0.28 (0.11)	0.39 (0.26)	0.06 (0.01)	8.129 (0.048)	2414 (18)	1822 (41)	240 (13)	3.72 (0.18)	2073 (31)	450 (73)
Nearshore exposed / summer	31.5 (0.6)	8.31 (0.12)	0.62 (0.25)	0.43 (0.15)	0.02 (0.02)	8.112 (0.024)	2346 (30)	1728 (32)	249 (12)	3.93 (0.19)	1988 (29)	467 (29)
Midshore sheltered / winter	25.9 (0.6)	8.00 (0.17)	0.35 (0.18)	0.64 (0.55)	0.07 (0.01)	8.123 (0.051)	2421 (21)	1835 (32)	236 (17)	3.65 (0.24)	2083 (21)	457 (74)
Midshore sheltered / summer	30.9 (0.6)	8.09 (0.22)	0.66 (0.24)	0.57 (0.26)	0.04 (0.02)	8.113 (0.031)	2365 (38)	1752 (41)	247 (14)	3.90 (0.23)	2011(37)	468 (41)
Midshore exposed / winter	26.1 (0.5)	8.15 (0.07)	0.27 (0.20)	0.34 (0.17)	0.07 (0.02)	8.152 (0.031)	2428 (18)	1814 (24)	249 (9)	3.86 (0.13)	2074 (19)	420 (41)
Midshore exposed / summer	30.7 (0.7)	8.16 (0.09)	0.61 (0.24)	0.68 (0.49)	0.05 (0.07)	8.130 (0.018)	2373 (37)	1745 (32)	254 (12)	3.99 (0.19)	2009 (32)	446 (20)
Offshore exposed / winter	26.0 (0.4)	8.10 (0.05)	0.38 (0.21)	0.37 (0.37)	0.09 (0.02)	8.156 (0.020)	2429 (20)	1813 (19)	250 52)	3.87 (0.07)	2073 (20)	414 (285)
Offshore exposed / summer	30.8 (0.7)	8.12 (0.08)	0.57 (0.23)	0.50 (0.16)	0.03 (0.02)	8.152 (0.021)	2393 (33)	1734 (39)	266 (12)	4.20 (0.21)	2011 (35)	422 (24)

840

841

842 **Table 2. Net-accretion/erosion rates G_{net} in coral reefs along a cross-shelf gradient in the central Red Sea, cumulative over**
843 **6, 12, and 30 months.** G_{net} (kg m^{-2} y^{-1}) was calculated using weight gain/loss of limestone blocks deployed in the reef sites for 6,
844 12, and 30 months. Means per reef site and standard deviations in brackets. y = year

G_{net} (kg m^{-2} y^{-1})	Deployment time (months)		
Reef site	**6**	**12**	**30**
Nearshore sheltered	0.16 (0.09)	-0.2 (0.35)	-
Nearshore exposed	0.11 (0.07)	-0.61 (0.49)	-0.96 (0.75)
Midshore sheltered	0.13 (0.09)	0.06 (0.03)	-0.29 (0.12)
Midshore exposed	0.11 (0.16)	0.01 (0.07)	0.06 (0.12)
Offshore sheltered	0.03 (0.02)	-0.07 (0.07)	-
Offshore exposed	0.14 (0.11)	0.08 (0.09)	0.37 (0.08)

845

Biogeosciences Discuss., https://doi.org/10.5194/bg-2018-57
Manuscript under review for journal Biogeosciences
Discussion started: 28 February 2018

846 **Table 3. Reef carbonate budget estimates and contributing biotic variables (kg m^{-2} y^{-1}) along a cross-shelf gradient in the**
847 **central Red Sea.** Calcification rates of benthic calcifiers ($G_{benthos}$), net-accretion/erosion rates of reef substrate ($G_{netbenthos}$), and the
848 erosion rates of echinoids and parrotfishes (E_{echino}, E_{parrot}) contribute to the total carbonate budget (G_{budget}) in a reef site. Means per
849 site are shown and standard deviations are in brackets. The last row gives the means and standard deviations across all sites.

Reef	G_{budget}	$G_{benthos}$	$G_{netbenthos}$	E_{echino}	E_{parrot}
Nearshore exposed	-1.477 (1.748)	0.426 (0.149)	-0.315 (0.129)	-0.228 (0.189)	-1.36 (1.886)
Midshore sheltered	0.598 (0.368)	1.15 (0.222)	-0.027 (0.014)	-0.187 (0.193)	-0.338 (0.271)
Midshore exposed	1.02 (0.353)	1.762 (0.242)	0.009 (0.003)	-0.024 (0.04)	-0.727 (0.307)
Offshore exposed	2.443 (1.033)	2.812 (0.646)	0.094 (0.022)	-0.019 (0.003)	-0.444 (0.701)
Cross-shelf gradient	0.646 (1.734)	1.538 (0.958)	-0.06 (0.168)	-0.114 (0.159)	-0.717 (1.04)

850

Biogeosciences Discuss., https://doi.org/10.5194/bg-2018-57
Manuscript under review for journal Biogeosciences
Discussion started: 28 February 2018

851 **Table 4. Coefficients from Spearman rank order correlations for predictor variables vs. G_{net} and G_{budget}.** Correlations were
852 performed using 13 abiotic variables including inorganic nutrients and carbonate system values. G_{budget} was additionally correlated
853 with 13 biotic variables from the transect survey including parrotfish, sea urchin abundances, various calcifier categories as %
854 cover, and rugosity. For G_{net} analysis three biotic variables were included, i.e., parrot fish abundances, coralline algae, and algal
855 and sponge cover. G_{net} (= net-accretion/erosion rates of limestone blocks) and G_{budget} (= carbonate budget estimates). Correlates
856 are only shown, when Spearman's correlation coefficient $\rho \geq |0.60|$.

	G_{net}		G_{budget}	
Abiotic variables	**ρ**	***p***	**ρ**	***p***
Temperature mean	-0.74	< 0.01	-0.71	< 0.001
Temperature SD	-0.74	< 0.01	-0.71	< 0.001
$pH_{(continuous)}$ SD	-0.81	< 0.001	-0.65	< 0.001
pCO_2 mean	-0.81	< 0.001	-0.65	< 0.001
A_T mean	0.93	< 0.001	0.89	< 0.001
Ω_a mean	0.81	< 0.001	0.65	< 0.001
CO_3^2 mean	0.81	< 0.001	0.65	< 0.001
PO_4^{3-}mean	0.74	< 0.01	0.71	< 0.001
Biotic variables	**ρ**	***p***	**ρ**	***p***
Rugosity	-	-	0.67	< 0.001
% total hard coral	-	-	0.70	< 0.001
% calcareous crusts	0.81	< 0.001	0.69	< 0.001

857

Biogeosciences Discuss., https://doi.org/10.5194/bg-2018-57
Manuscript under review for journal Biogeosciences
Discussion started: 28 February 2018

858 **Table 5. Distance based linear models (DistLM) and sequential tests.** Response variables were G_{net} (net-accretion/erosion rates
859 of limestone blocks) and G_{budget} (reef carbonate budget estimates). Predictor variables were 13 abiotic variables including inorganic
860 nutrients and carbonate system values. The G_{net} model was added three biotic variables, i.e., parrot fish abundances, coralline algae
861 cover, and algal and sponge cover. In the G_{budget} model 13 biotic transect variables were included, such as parrotfish, sea urchin
862 abundances, various calcifier categories as % cover, and rugosity. Significant predictors in **bold**.

RESPONSE VARIABLE: G_{net}							
Best Model	**Adj R^2**	**R^2**	**RSS**	**# of fitted Variables**			
	0.65	0.67	1.90	1			
Sequential test							
Variable	**Cumul. Adj R^2**	**SS (trace)**	**Pseudo-F**	***p***	**R^2.**	**Cumul. R^2**	**res.df**
+A_T mean	**0.65**	**3.84**	**28.30**	**0.00**	**0.67**	**0.67**	**14**
RESPONSE VARIABLE: G_{budget}							
Best Model	**Adj R^2**	**R^2**	**RSS**	**# of fitted Variables**			
	0.81	0.84	11.123	4			
Sequential test							
Variable	**Cumul. Adj. R^2**	**SS (trace)**	**Pseudo-*F***	***p***	**R^2**	**Cumul. R^2**	**res.df**
+A_T mean	**0.64**	**45.44**	**42.09**	**0.000**	**0.66**	**0.66**	**22**
+Parrotfish abundance	**0.78**	**10.15**	**15.67**	**0.001**	**0.15**	**0.80**	**21**
+ $pH_{(continuous)}$ SD	0.79	1.09	1.74	0.208	0.02	0.82	20
+% encrusting coral	0.81	1.39	2.37	0.142	0.02	0.84	19

863 Cumul. Adj. R^2 = Cumulative adjusted R^2, Cumul. R^2 = Cumulative R^2, res.df = residual degrees of freedom, A_T = total alkalinity

864

Biogeosciences Discuss., https://doi.org/10.5194/bg-2018-57
Manuscript under review for journal Biogeosciences
Discussion started: 28 February 2018

865 **Table 6. Global comparison of the carbonate system for coral reefs.**

	A_T (µmol kg^{-1})	Ω_a	pCO_2 (µatm)
Central Red Sea (this study)[1]	2346 – 2429	3.65 – 4.20	414 – 468
Global pre-industrial values (Manzello et al., 2008)[2]	~2315	~4.3	~280
Great Barrier Reef (Uthicke et al., 2014)[3]	2069-2315	2.6-3.8	340-554
Puerto Rico, Caribbean (Gray et al., 2012)[4]	2223-2315	3.4-3.9	356-460
Bermuda (Yeakel et al., 2015) [5]	2300-2400	2.7-3.6	300-450
Panama, upwelling sites (Manzello et al., 2008) [2]	1869.5	2.96	368
Galapagos (Manzello et al., 2008)[2]	2299	2.49	636

866 [1] lowest and highest means per reef site and season; [2] estimated averages, for details see referenced study; [3] lowest and highest means
867 from reef sites during wet and dry seasons; [4] lowest and highest seasonal means from one site; [5] minimum and maximum from time
868 series plots